J. Fluid Mech. (2011), *vol.* 667, *pp.* 426–462.
doi:10.1017/S0022112010004532

Acoustic/steady streaming from a motionless boundary and related phenomena: generalized treatment of the inner streaming and examples

A. Y. REDNIKOV† AND S. S. SADHAL‡

Department of Aerospace and Mechanical Engineering, University of Southern California, Los Angeles, CA 90089-1453, USA

(Received 7 August 2010; revised 7 August 2010; accepted 20 August 2010)

As originally realized by Nyborg (*J. Acoust. Soc. Am.*, vol. 30, 1958, p. 329), the problem of the inner acoustic/steady streaming can be analysed in quite general terms. The inner streaming is the one that develops in the high-frequency limit in a thin Stokes (shear-wave) layer at a boundary, in contrast to the outer streaming in the main bulk of the fluid. The analysis provides relevant inner-streaming characteristics through a given distribution of the acoustic amplitude along the boundary. Here such a generalized treatment is revisited for a motionless boundary. By working in terms of surface vectors, though in elementary notations, new compact and easy-to-use expressions are obtained. The most important ones are those for the effective (apparent) slip velocity at the boundary as seen from a perspective of the main bulk of the fluid, which is often the sole driving factor behind the outer streaming, and for the induced (acoustic) steady tangential stress on the boundary. As another novel development, non-adiabatic effects in the Stokes layer are taken into account, which become apparent through the fluctuating density and viscosity perturbations, and whose contribution into the streaming is often ignored in the literature. Some important particular cases, such as the axisymmetric case and the incompressible case, are emphasized. As far as the application of the derived general inner-streaming expressions is concerned, a few examples provided here involve a plane acoustic standing wave, which either grazes a wall parallel to its direction (convenient for the estimation of the non-adiabatic effects), or into which a small (compared to the acoustic wavelength) rigid sphere is placed. If there are simultaneously two such waves, out-of-phase and, say, in mutually orthogonal directions, a disk placed coplanarly with them will undergo a steady torque, which is calculated here as another example. Two further examples deal with translational high-frequency harmonic vibrations of particles relative to an incompressible fluid medium, *viz.* of a rigid oblate spheroid (along its axis) and of a sphere (arbitrary three dimensional). The latter can be a fixed rigid sphere, one free to rotate or even a (viscous) spherical drop, for which the outer streaming and the internal circulation are also considered.

Key words: acoustics, particle/fluid flows, Stokesian dynamics

† Present address: TIPs – Fluid Physics, Université Libre de Bruxelles, CP 165/67, 50 Av. F. D. Roosevelt, 1050 Brussels, Belgium.

‡ Email address for correspondence: sadhal@usc.edu

1. Introduction

A mean flow appearing on the background of a small-amplitude oscillatory flow is often referred to as 'acoustic streaming'. The term is coined under the premise that the oscillatory flow in question is attributable to an acoustic wave. Nonetheless, the phenomenon can occur and is of interest in intrinsically incompressible situations (when the acoustic wavelength is much greater than the length scale of the problem). In such a case, the term 'steady streaming' seems to be more appropriate (Riley 2001). In any event, of interest is mainly the high-frequency limit, when the typical viscous time is much greater than the oscillation period. It is in this limit that significant streaming flows arise, which may be characterized by large Reynolds numbers in spite of a small amplitude of the primary oscillatory flow. On the contrary, if the frequency is not high, the streaming flows are typically weak, and the Reynolds number is small (Riley 1966). It is the high-frequency limit that is meant hereafter in the present paper.

For an extensive review of the phenomenon of acoustic streaming, we refer the reader to Nyborg (1965, 1998) and Riley (1967, 1997, 2001). Two types of acoustic streaming are usually distinguished (Riley 1997, 2001): type I ('quartz wind') and type II (the Rayleigh streaming). The distinction basically owes itself to the high-frequency limit, and would not make sense otherwise. In this limit, the primary oscillatory flow is irrotational (to leading order) in the main bulk of the fluid, while the oscillatory vorticity is confined to the oscillatory boundary layer (the Stokes layer) at walls and interfaces. Now the type I streaming is the one which is generated in the main bulk, while the type II streaming is generated in the Stokes layer (although it is not confined to it and rather spreads into the main bulk). Vorticity, along with nonlinearity, is the primary factor behind the steady flow generation (in contrast to merely generating an effective 'hydrostatic' pressure distribution, often referred to as 'radiation pressure', which is mainly responsible for steady forces acting on particles in an acoustic field). Thus, the generation is much stronger (as per unit volume) in the Stokes layer. But this by no means implies that the type II streaming is necessarily stronger though: it gets slowed down by the boundary, and more importantly, the overall effect may be greatly enhanced for the type I streaming due to a much larger volume of the main bulk.

As an example of the situation when the type I streaming is predominant, let us point out irradiation of an acoustic beam into a large volume of fluid. For high-intensity ultrasound beams, the resulting 'quartz wind' is rather appreciable (Lighthill 1978). On the other hand, when the primary oscillatory flow is all in phase (to leading order) as in an acoustic standing wave, the type II streaming tends to dominate, as first studied by Rayleigh (1883). In the incompressible case, the type I streaming is absent, and the streaming is entirely of type II.

Another type of streaming is what Lighthill (1978) refers to as 'McIntyre streaming'. This is essentially a 'kinematic' type of streaming, caused by oscillations of a boundary normal to itself. For a non-trivial result, it is essential that phase differences exist in the primary oscillatory flow. The streaming due to surface waves in liquid layers (see Riley 2001) can be ascribed to this same type. In the present paper, the consideration is limited to motionless boundaries.

The boundary-layer structure of the primary oscillatory flow, with the zones of the Stokes layer and the main bulk distinguished, is carried over to the streaming flow. Accordingly, one distinguishes between the 'inner' (near-boundary) streaming in the Stokes layer, and the 'outer' streaming in the main bulk. As already mentioned, while the type II streaming originates in the Stokes layer, it cannot be confined to that region and engages the main bulk too. In terms of the inner and outer streaming, this

means that the inner streaming does not fade away at the outer edge of the Stokes layer. Rather (here it is assumed that the boundary is motionless), it tends to a finite velocity value, tangential (to leading order) to the boundary in view of the thinness of the Stokes layer. Due to the latter reason, it is seen as an effective (apparent) slip velocity distribution at the boundary itself from the viewpoint of the main bulk. It can be said that it is the effective slip velocity that causes the type II outer streaming near a motionless boundary. To leading order, the inner streaming is generally independent of the outer streaming, irrespective of whether the latter is type I, type II, or both. Apart from the already mentioned effective slip velocity, another important feature of the inner streaming is the steady tangential stress exerted upon the boundary. As the steady velocity profile varies sharply across the thin Stokes layer, the stress due to the inner streaming is generally much greater than what could ever be exerted by an outer streaming of the same intensity.

Nyborg (1958) realized that consideration of the inner streaming can be carried out in quite general terms for an arbitrary smooth boundary. As the result, characteristics of the inner streaming and the effective streaming velocity, in particular (even though he does not work in such terms), are expressed through the distribution of the amplitude of the primary oscillatory flow along the boundary and the geometric properties of the latter. A simpler, one-dimensional result of this kind is mentioned in Riley (2001) for the incompressible case. A quasi-two-dimensional result is provided by Lighthill (1997). Lee & Wang (1989) revisit Nyborg's generalized treatment, correct certain points, and apply it to describing the streaming from a rigid sphere fixed in two out-of-phase orthogonal acoustic standing waves. The treatment of Lee & Wang (1989), just as the original one of Nyborg (1958), explicitly represents it all in terms of an orthogonal curvilinear coordinate system introduced on the boundary. The result looks rather cumbersome. It seems that a more compact, clear-cut and easy-to-use representation can be achieved if the vector notation is kept through. One of the goals of the present paper is to realize such a representation for the inner streaming near a motionless boundary. After the generalized result is obtained, certain particular cases as well as application to specific problems are considered.

Compressibility and adiabaticity are two controversial issues related to the inner-streaming treatment. Landau & Lifshitz (1988, see § 80 therein) proceed in an essentially compressible situation as if the primary oscillatory flow were incompressible in the Stokes layer, which is not correct. Nonetheless, the final result for the outer streaming (and thus for the effective slip velocity, although they do not work in such terms) happens to be correct in the sense that one comes up with the same result if the primary oscillatory flow in the Stokes layer is treated as compressible and adiabatic. In fact, it *is* considered compressible and adiabatic by Nyborg (1958) and Lee & Wang (1990), as well as by Zhao, Sadhal & Trinh (1999*b*). However, there comes another issue. Unlike the main bulk, the dissipative effects do matter in the Stokes layer, and thus the entropy being constant therein may not be a solid assumption. The non-adiabatic effect on the streaming is considered by Gopinath & Trinh (2000) for a particular problem of a sphere in a standing wave. In the present paper, the non-adiabatic effect is incorporated within the generalized treatment of the inner streaming.

Another issue often ignored when calculating the inner streaming is that the coefficient of viscosity is a function of state, and not merely a constant. The associated effect of such viscosity variability on the inner streaming is comparable with that due to compressibility. It *is* ignored in the above cited studies. Yarin *et al.* (1999) take it

into account, albeit in the adiabatic framework. In the present paper, it is incorporated non-adiabatically.

The paper is organized into two parts as follows. The first part (§ 2) is dedicated to a generalized treatment of the inner streaming along the lines described above, and formulas for the effective slip velocity and the induced steady tangential stress on the boundary are derived. At the end of § 2, these are specified for two important particular situations, which are the incompressible case, on the one hand, and the plane and axisymmetric geometry, on the other. *A practical summary of the most important results of* § 2 *is provided in* § 2.12. The second part (§ 3) illustrates with examples the application of the general results of § 2 to concrete problems. The problems chosen as the examples for § 3 have already been considered in one form or another in the literature, although for nearly all of them the present analysis also yields a number of new results.

A few of the examples involve a plane acoustic standing wave. In particular, the classical problem of a standing wave grazing a parallel wall is revisited, which is mainly with the purpose of estimating the importance of the newly incorporated non-adiabatic effects (§ 3.1).

Next, the streaming from a small (as compared to the acoustic wavelength) rigid sphere placed at an arbitrary position within the standing wave is considered (§ 3.2). The result is presented as an expansion in terms of a small parameter, the latter being the acoustic wavenumber scaled with the sphere radius (the dimensionless wavenumber) and the leading order corresponding to the incompressible limit. The analysis here goes one step further than just deriving the effective slip velocity on the sphere starting from the formulas of § 2: the associated outer streaming is also calculated, albeit only in the Stokes approximation. What we eventually come up with in § 3.2 generalizes certain results from the literature. In particular, as compared to Lee & Wang (1990) and Zhao *et al.* (1999*b*), the non-adiabatic effects are taken into account and besides a leading-order result for the streaming which is uniformly valid for all positions of the sphere within the standing wave (including the velocity node) is constructed. As compared to Gopinath & Trinh (2000), the viscosity variability (non-adiabatic) is additionally taken into account, even though fewer terms of the expansion are eventually retained.

A similar problem for an oblate spheroid (§ 3.3) is partly inspired by the fact that acoustically levitated drops assume an oblate shape (Marston 1980; Lee, Anikumar & Wang 1994; Yarin, Pfaffenlehner & Tropea 1998). Yet the analysis is limited here to the leading order in the dimensionless acoustic wavenumber (scaled with the spheroid size). In this way, the problem is equivalent to that of an incompressible fluid medium oscillating relative to an oblate spheroid along its axis studied by Rednikov & Sadhal (2004). In essence, the goal of § 3.3 is just to show how easily the expression for the effective slip velocity derived by Rednikov & Sadhal (2004) in a direct way can be recovered using the formulas of § 2. For the analysis of the outer streaming engendered by this slip velocity, the reader is relegated to Rednikov & Sadhal (2004). Let us also mention a recent experimental study of steady streaming from oscillating spheroids (Kotas, Yoda & Rogers 2007).

As the example chosen for § 3.4, a sphere placed into an incompressible fluid medium undergoing a three-dimensional (generally, non-uniaxial) translational oscillation is considered. One possible interpretation is that the sphere is within two out-of-phase orthogonal acoustic standing waves with the wavelength much greater than the sphere radius (the incompressible limit). As compared to Lee & Wang (1989), where this problem has been originally treated, one can fully appreciate the advantage of a

vector-form representation. Further, as far as the extension of the analysis to the outer streaming is concerned, treated here is not only the problem of a 'fixed' rigid sphere as in Lee & Wang (1989), but also a sphere free to rotate and its generalization to a spherical drop (although its dynamic viscosity is required in the analysis to be much greater than that of the medium, e.g. a drop in air) including the internal circulation. The latter part is also a generalization of the earlier studies that have considered more particular forms of a translational oscillation than that is here: uniaxial (Zhao, Sadhal & Trinh 1999*a*) and of circular-polarization type (Rednikov, Riley & Sadhal 2003). There is a recent experimental interest in studying steady streaming from oscillating spheres (Otto, Riegler & Voth 2008), although the mentioned study corresponds to different conditions from those implied here.

In § 3.5, as a final example, the results of § 2 are applied to calculating the steady torque on a thin disk in two orthogonal standing waves with a phase difference. The disk is oriented coplanarly with the directions of the waves. As compared to Busse & Wang (1981), the non-adiabatic effects are also taken into account.

Finally, concluding remarks are provided in § 4.

2. Generalized treatment

2.1. *Statement of the problem and assumptions*

We consider a situation when an acoustic field of a given frequency ω^* exists in the vicinity of a motionless rigid surface (boundary). Let l^* be the length scale of the problem, which can be either the typical radius of curvature of the surface or the acoustic wavelength, whichever is smaller. The general case corresponds to these two being of the same order, i.e. to the dimensionless wavenumber

$$k = k^* l^* \tag{2.1}$$

being of order unity, where $k^* = \omega^*/c^*$ is the wavenumber while c^* is the speed of sound. The incompressible limit $k \ll 1$ can then be treated as a particular case.

Now if U^* is a quantity of the order of the velocity amplitude in the acoustic wave and ν^* is the kinematic viscosity of the fluid (in the unperturbed state), we assume that

$$\varepsilon = \frac{U^*}{\omega^* l^*} \ll 1, \qquad M^2 = \frac{\omega^* l^{*2}}{\nu^*} \gg 1, \tag{2.2}$$

which are the small-amplitude and the high-frequency assumptions, respectively. We note that ε is actually an inverse Strouhal number, εk is the Mach number; M will be referred to as the frequency parameter. In view of (2.2), to leading order, the acoustic field is ideal, in the sense that it is described by linear acoustics, and is irrotational and isentropic in the main bulk of the fluid, outside the oscillatory boundary layer (the Stokes layer). The thickness of the latter is $O(l^*/M)$, which is much smaller than l^*. In the Stokes layer, the dissipative effects are important, and the oscillatory flow is rotational with the oscillatory vorticity decaying exponentially at the outer edge. Now if nonlinear effects are taken into consideration, it makes for a relatively intense localized generation of a steady flow component (acoustic or steady streaming) in the Stokes layer, though the steady flow itself is ultimately not localized therein. In this section, assuming that the ideal acoustic field is known at the surface, we provide a generalized treatment of steady streaming in the Stokes layer (the inner streaming). The flow field in the two regions (main bulk and the Stokes layer) is treated by means of matched asymptotic expansions.

The nonlinear effects that lead to acoustic streaming are usually associated with the action of the Reynolds stresses. However, there is another nonlinear contribution, which is due to viscosity fluctuation in the acoustic wave. In the Stokes layer, where the viscous effect is of the leading order, it may be comparable to the one due to the Reynolds stresses. In the present paper, this effect is taken into consideration. Thus, one of the variables we have to follow is the viscosity perturbation upon the background value.

Another condition to be taken into account here is that temperature is among the fluctuating quantities in the acoustic wave. To the extent that the Stokes layer is a viscous oscillatory boundary layer, it is a thermal one as well (assuming here that the Prandtl number is of order unity). Then the oscillatory temperature profile in the Stokes layer may significantly depart from the isentropic one, unless the boundary is insulating. This may bring about a contribution towards the streaming by means of the temperature dependence of the fluid density and viscosity. We refer to this contribution as the non-adiabatic effect.

2.2. *Non-dimensionalization and some basic notations*

The following convention is used throughout the paper: dimensional quantities are marked with an asterisk (not the dimensionless ones). If f^* is a dimensional quantity whose dimensionless counterpart f is defined (and *vice versa*), then the notation $[f]$ refers to the scale of f, i.e.

$$f^* = [f]\, f. \tag{2.3}$$

For example, $[k] = 1/l^*$, cf. (2.1). For many dimensional quantities, no dimensionless counterpart is ever defined, as e.g. for those on the right-hand side of (2.2). Nonetheless, to avoid confusion, they still carry an asterisk. Other quantities may be defined as genuinely dimensionless, as e.g. the numbers ε and M in (2.2). For these, the paradigm (2.3) is not applicable.

The following notations are introduced: t (time), $\boldsymbol{r}$ (position vector), y (for any given point in space, the normal distance to the boundary), ∇ (gradient operator), $\boldsymbol{v}$ (velocity field in the main bulk), $\boldsymbol{V}$ (velocity field in the Stokes layer), p (pressure perturbation, upon the background value, in the main bulk), $\mathscr{P}$ (pressure perturbation in the Stokes layer), $\boldsymbol{\sigma}_{ts}$ (tangential stress on the boundary). In addition, $\mathscr{R}$, $\mathscr{N}$ and $\mathscr{T}$ are the density, the dynamic-viscosity and the temperature perturbations (upon the corresponding background values). These latter quantities are considered only in the Stokes layer. In certain examples treated in the present paper, the net viscous torque $\boldsymbol{\Gamma}$ acting on a body and the angular velocity of rotation $\boldsymbol{\Omega}$ are considered, and the velocity potential φ and the axisymmetric stream function ψ are introduced. The scales used are

$$[t] = 1/\omega^*,\ \ [\boldsymbol{r}] = [y] = l^*,\ \ [\nabla] = 1/l^*,\ \ [\boldsymbol{v}] = [\boldsymbol{V}] = U^*, \tag{2.4}$$

$$[p] = [\mathscr{P}] = \rho^*\omega^* l^* U^*,\ \ [\mathscr{R}] = \rho^*\omega^* l^* U^*/c^{*2},\ \ [\mathscr{N}] = \eta^*\omega^* l^* U^*/c^{*2}, \tag{2.5}$$

$$[\mathscr{T}] = \left(\frac{\partial T^*}{\partial P^*}\right)_{S^*}[\mathscr{P}] = \frac{T^*\beta^*}{c_p^*\,\rho^*}\,[\mathscr{P}] = \frac{T^*\beta^*\omega^* l^* U^*}{c_p^*}, \tag{2.6}$$

$$[\boldsymbol{\sigma}_{ts}] = [p]/M = \rho^*\omega^* l^* U^*/M,\ \ [\boldsymbol{\Gamma}] = [\boldsymbol{\sigma}_{ts}]\, l^{*3} = \rho^*\omega^* l^{*4} U^*/M, \tag{2.7}$$

$$[\boldsymbol{\Omega}] = U^*/l^*,\ \ [\varphi] = U^* l^*,\ \ [\psi] = U^* l^{*2}, \tag{2.8}$$

where the quantities not yet defined are the following: ρ^* (density of the fluid), P^* (pressure), $\eta^* = \rho^*\nu^*$ (dynamic viscosity), T^* (absolute temperature), c_p^* (specific heat

at constant pressure), S^* (entropy) and β^* (thermal expansion coefficient),

$$\beta^* = -\frac{1}{\rho^*}\left(\frac{\partial \rho^*}{\partial T^*}\right)_{P^*}. \tag{2.9}$$

Here the thermodynamic properties and the viscosity are taken for the unperturbed (background) state of the fluid.

2.3. *Unsteady/steady parts and other basic conventions*

Any relevant flow characteristic f (e.g. the velocity field) is represented as a sum of the unsteady and the steady parts

$$f = f^{(u)}(t) + \langle f \rangle. \tag{2.10}$$

Here $f^{(u)}$ is the unsteady (fluctuating, oscillatory) part of f, with the superscript '(u)' referring to 'unsteady'. Further, $\langle \cdots \rangle$ denotes the time average (at a given spatial point for the field quantities), and $\langle f \rangle$ is the steady part. Furthermore, the steady part is rescaled with the small parameter ε as

$$\langle f \rangle = \varepsilon\, f^{(s)}. \tag{2.11}$$

For most steady quantities studied in the present paper, one has $\langle f \rangle = O(\varepsilon)$ indeed, so that $f^{(s)} = O(1)$, which justifies the rescaling (2.11). In any event, the steady part is always assumed to be small enough here, so that the problem governing the unsteady part can be linearized just around the unperturbed state of the fluid (to leading order). Whenever a quantity with the superscript '(s)' is encountered, it is understood in the sense of (2.11). The superscript '(s)' refers to 'steady'. It is the steady part that is the primary focus of the present paper.

For the unsteady part, we have

$$f^{(u)} = \mathrm{Re}\left\{ f^{(u1)} \mathrm{e}^{\mathrm{i}t} \right\} \tag{2.12}$$

to leading order, where $\mathrm{Re}\{\cdots\}$ denotes the real part of the expression ($\mathrm{Im}\{\cdots\}$ will correspond to the imaginary part). Whenever the superscript '$(u1)$' is used, it refers to the corresponding complex amplitude, just as $f^{(u1)}$ in (2.12). Higher-order harmonics (double, triple frequency, etc., with the complex amplitudes $f^{(u2)}$, $f^{(u3)}, \ldots$) are generated due to nonlinearity. However, they are asymptotically small, and they will not be considered in the framework of the present paper. Hereafter, the complex conjugate is denoted by an overbar, e.g.

$$\overline{f^{(u1)}}. \tag{2.13}$$

In the notations introduced, equations satisfied by the primary oscillatory flow (due to the acoustic wave) in the main bulk can be written as

$$k^2\, \mathrm{i}\, p^{(u1)} + \nabla \cdot \boldsymbol{v}^{(u1)} = 0, \quad \mathrm{i}\, \boldsymbol{v}^{(u1)} = -\nabla p^{(u1)}, \tag{2.14}$$

$$\boldsymbol{v}^{(u1)} \cdot \boldsymbol{n} = 0 \quad \text{at the surface.} \tag{2.15}$$

Here $\boldsymbol{n}$ is the unit vector normal to the boundary (and pointing towards the fluid).

For any spatial point, if y is the normal distance to the surface and Q_s is the surface point at the base of the normal emitted from this spatial point to the surface, the position vector can be represented as

$$\boldsymbol{r} = \boldsymbol{r}_s(Q_s) + y\, \boldsymbol{n}(Q_s), \tag{2.16}$$

where $\boldsymbol{r}_s$ is the position vector for the surface points. Now if a coordinate system $\{\xi, \eta\}$ is introduced on the surface, so that $Q_s = \{\xi, \eta\}$, then (2.16) defines a curvilinear coordinate system $\{\xi, \eta, y\}$ in space.

For the purpose of using the boundary-layer approximation in the Stokes layer, it is convenient to decompose the gradient operator and a typical vector field $\boldsymbol{a}$ into the tangential and the normal components. We write

$$\nabla_\tau = \nabla - \boldsymbol{n}\,\boldsymbol{n}\cdot\nabla, \quad \frac{\partial}{\partial y} = \boldsymbol{n}\cdot\nabla, \tag{2.17}$$

$$\boldsymbol{a}_\tau = \boldsymbol{a} - \boldsymbol{n}\,\boldsymbol{n}\cdot\boldsymbol{a}, \quad a_n = \boldsymbol{n}\cdot\boldsymbol{a}, \tag{2.18}$$

with the subscripts 'τ' and 'n' referring to the tangential and the normal components, respectively. At each spatial point, the vector $\boldsymbol{n}$ is the same as at the base of the normal from this point to the surface

$$\frac{\partial \boldsymbol{n}}{\partial y} = \boldsymbol{0}. \tag{2.19}$$

Hereinafter, the subscript 's' will be used to indicate that a given quantity is evaluated at or belongs to the surface (boundary). For instance,

$$\nabla_{\tau s} \equiv \nabla_\tau|_{surface}, \quad \boldsymbol{v}_{\tau s}^{(u1)} \equiv \boldsymbol{v}_\tau^{(u1)}\big|_{surface}, \quad p_s^{(u1)} \equiv p^{(u1)}\big|_{surface}. \tag{2.20}$$

In the Stokes layer, the normal coordinate y is of the order $O(M^{-1})$. Therefore, it is convenient to rescale it as

$$Y = y\,M, \tag{2.21}$$

so that $Y = O(1)$.

At the same time, for the velocity field $\boldsymbol{V}$ in the Stokes layer we expect $V_n = O(M^{-1})$, whereas $\boldsymbol{V}_\tau = O(1)$. Thus, the normal velocity component is similarly rescaled as

$$V_Y = V_n\,M, \tag{2.22}$$

so that $V_Y = O(1)$.

2.4. *Leading-order boundary-layer equations in the Stokes layer*

When considering the flow field in the Stokes layer, the boundary-layer approximation is applicable. For the continuity, tangential and normal momentum equations, we have (see Rosenhead 1963, pp. 411–415)

$$k^2\frac{\partial \mathscr{R}}{\partial t} + \nabla_{\tau s}\cdot\boldsymbol{V}_\tau + \frac{\partial V_Y}{\partial Y} + \varepsilon\,k^2\left(\nabla_{\tau s}\cdot\mathscr{R}\boldsymbol{V}_\tau + \frac{\partial \mathscr{R} V_Y}{\partial Y}\right) = 0, \tag{2.23}$$

$$(1+\varepsilon\,k^2\mathscr{R})\left(\frac{\partial \boldsymbol{V}_\tau}{\partial t} + \varepsilon[\boldsymbol{V}_\tau\cdot\nabla_{\tau s}\boldsymbol{V}_\tau]_\tau + \varepsilon\,V_Y\frac{\partial \boldsymbol{V}_\tau}{\partial Y}\right) = -\nabla_{\tau s}\mathscr{P} + \frac{\partial^2 \boldsymbol{V}_\tau}{\partial Y^2} + \varepsilon\,k^2\frac{\partial}{\partial Y}\left(\mathscr{N}\frac{\partial \boldsymbol{V}_\tau}{\partial Y}\right), \tag{2.24}$$

$$0 = \frac{\partial \mathscr{P}}{\partial Y}. \tag{2.25}$$

Here $[\cdots]_\tau$ denotes the tangential component of the corresponding term. The difference between ∇_τ and $\nabla_{\tau s}$ is negligible to leading order.

2.5. *Primary oscillatory flow in the Stokes layer – part 1*

The unsteady part satisfies linearized versions of (2.23)–(2.25). In terms of the complex amplitudes (2.12), we have

$$\mathrm{i}\,k^2\mathscr{R}^{(u1)} + \nabla_{\tau s}\cdot\boldsymbol{V}_\tau^{(u1)} + \frac{\partial V_Y^{(u1)}}{\partial Y} = 0, \tag{2.26}$$

$$\mathrm{i}\,\boldsymbol{V}_\tau^{(u1)} = -\nabla_{\tau s}\mathscr{P}^{(u1)} + \frac{\partial^2\boldsymbol{V}_\tau^{(u1)}}{\partial Y^2}, \tag{2.27}$$

$$0 = \frac{\partial\mathscr{P}^{(u1)}}{\partial Y}. \tag{2.28}$$

The no-slip and the non-penetration conditions at the surface are

$$\boldsymbol{V}_\tau^{(u1)} = \boldsymbol{0}, \quad V_Y^{(u1)} = 0 \qquad \text{at } Y = 0, \tag{2.29}$$

and the conditions of matching with the flow field in the main bulk (presumed to be known here) are

$$\boldsymbol{V}_\tau^{(u1)} \to \boldsymbol{v}_{\tau s}^{(u1)}, \quad \mathscr{P}^{(u1)} \to p_s^{(u1)} \quad \text{as } Y \to \infty, \tag{2.30}$$

where the use of the subscript 's' (see § 2.3) should be noted. Here

$$\mathrm{i}\,\boldsymbol{v}_{\tau s}^{(u1)} = -\nabla_{\tau s}p_s^{(u1)} \tag{2.31}$$

in view of (2.14).

The solution of (2.27)–(2.30) for the pressure and the tangential velocity is

$$\mathscr{P}^{(u1)} = p_s^{(u1)}, \tag{2.32}$$

$$\boldsymbol{V}_\tau^{(u1)} = \boldsymbol{v}_{\tau s}^{(u1)}\{1 - \mathrm{e}^{-\sqrt{\mathrm{i}}\,Y}\}, \tag{2.33}$$

where $\sqrt{\mathrm{i}} = (1+\mathrm{i})/\sqrt{2}$. The solution for the density and viscosity perturbations and the normal velocity will be provided later, after considering the constitutive relations for the fluid. A noteworthy feature of the tangential velocity field (2.33) here is that it is surface-potential (representable as $\nabla_{\tau s}$ applied to a scalar function), as evident from (2.31).

2.6. *Steady formulation in the Stokes layer*

In accordance with the scaling (2.11), we write

$$\langle\boldsymbol{V}_\tau\rangle = \varepsilon\,\boldsymbol{V}_\tau^{(s)}, \quad \langle\mathscr{P}\rangle = \varepsilon\,\mathscr{P}^{(s)}. \tag{2.34}$$

The leading-order result of applying $\langle\cdots\rangle$ to (2.24) is

$$k^2\left\langle\mathscr{R}^{(u)}\frac{\partial\boldsymbol{V}_\tau^{(u)}}{\partial t}\right\rangle + \frac{1}{2}\nabla_{\tau s}\left\langle\boldsymbol{V}_\tau^{(u)}\cdot\boldsymbol{V}_\tau^{(u)}\right\rangle + \left\langle V_Y^{(u)}\frac{\partial\boldsymbol{V}_\tau^{(u)}}{\partial Y}\right\rangle = -\nabla_{\tau s}\mathscr{P}^{(s)} + \frac{\partial^2\boldsymbol{V}_\tau^{(s)}}{\partial Y^2} + k^2\frac{\partial}{\partial Y}\left\langle\mathscr{N}^{(u)}\frac{\partial\boldsymbol{V}_\tau^{(u)}}{\partial Y}\right\rangle. \tag{2.35}$$

The second term on the right-hand side has been rewritten using the property

$$[\boldsymbol{a}_\tau\cdot\nabla_\tau\boldsymbol{a}_\tau]_\tau = \tfrac{1}{2}\nabla_\tau(\boldsymbol{a}_\tau\cdot\boldsymbol{a}_\tau) \tag{2.36}$$

of a surface-potential vector field $\boldsymbol{a}_\tau$ (see the Appendix), which is applicable here in view of (2.33) and (2.31).

The first term in (2.35) can be rearranged in a different way. We write

$$k^2\left\langle \mathscr{R}^{(u)}\frac{\partial \boldsymbol{V}_\tau^{(u)}}{\partial t}\right\rangle = -k^2\left\langle \boldsymbol{V}_\tau^{(u)}\frac{\partial \mathscr{R}^{(u)}}{\partial t}\right\rangle = \left\langle \boldsymbol{V}_\tau^{(u)}\nabla_{\tau s}\cdot \boldsymbol{V}_\tau^{(u)}\right\rangle + \left\langle \boldsymbol{V}_\tau^{(u)}\frac{\partial V_Y^{(u)}}{\partial Y}\right\rangle, \tag{2.37}$$

where the second equality follows from the linearized version of the continuity equation (2.23). Thus, (2.35) can be rewritten as

$$\frac{1}{2}\nabla_{\tau s}\left\langle \boldsymbol{V}_\tau^{(u)}\cdot \boldsymbol{V}_\tau^{(u)}\right\rangle + \left\langle \boldsymbol{V}_\tau^{(u)}\nabla_{\tau s}\cdot \boldsymbol{V}_\tau^{(u)}\right\rangle + \frac{\partial}{\partial Y}\left\langle V_Y^{(u)}\boldsymbol{V}_\tau^{(u)}\right\rangle = -\nabla_{\tau s}\mathscr{P}^{(s)} + \frac{\partial^2 \boldsymbol{V}_\tau^{(s)}}{\partial Y^2} + k^2\frac{\partial}{\partial Y}\left\langle \mathscr{N}^{(u)}\frac{\partial \boldsymbol{V}_\tau^{(u)}}{\partial Y}\right\rangle. \tag{2.38}$$

In terms of the complex amplitudes (2.12), (2.38) becomes

$$\frac{1}{4}\nabla_{\tau s}\left(\boldsymbol{V}_\tau^{(u1)}\cdot\overline{\boldsymbol{V}_\tau^{(u1)}}\right) + \frac{1}{2}\mathrm{Re}\left\{\boldsymbol{V}_\tau^{(u1)}\nabla_{\tau s}\cdot\overline{\boldsymbol{V}_\tau^{(u1)}}\right\} + \frac{1}{2}\frac{\partial}{\partial Y}\mathrm{Re}\left\{V_Y^{(u1)}\overline{\boldsymbol{V}_\tau^{(u1)}}\right\} = -\nabla_{\tau s}\mathscr{P}^{(s)} + \frac{\partial^2 \boldsymbol{V}_\tau^{(s)}}{\partial Y^2} + \frac{1}{2}k^2\frac{\partial}{\partial Y}\mathrm{Re}\left\{\mathscr{N}^{(u1)}\frac{\partial\overline{\boldsymbol{V}_\tau^{(u1)}}}{\partial Y}\right\}, \tag{2.39}$$

where the overbar denotes the complex conjugate, as mentioned earlier.

From (2.25), one has

$$\frac{\partial \mathscr{P}^{(s)}}{\partial Y} = 0. \tag{2.40}$$

For a motionless boundary, a no-slip condition is imposed

$$\boldsymbol{V}_\tau^{(s)} = \boldsymbol{0} \quad \text{at } Y = 0, \tag{2.41}$$

whereas at $Y \to \infty$, the minimal possible singularity in the solution for $\boldsymbol{V}_\tau^{(s)}$ is required, which in particular will prove sufficient for determining the steady pressure $\mathscr{P}^{(s)}$.

In principle, for certain applications it may be useful to allow for a non-zero steady velocity at the boundary, even though still assuming it to be motionless with regard to the primary oscillatory flow as specified in (2.29). Then, instead of (2.41), we have

$$\boldsymbol{V}_\tau^{(s)} = \boldsymbol{u}_\tau^{(s)} \quad \text{at } Y = 0, \tag{2.42}$$

where $\boldsymbol{u}_\tau^{(s)}$ is regarded as being given within the problem (2.39), (2.40) and (2.42). From the form of (2.39), it is evident that the modification from (2.41) to (2.42) will merely result in a trivial addition of a constant (across the layer) term $\boldsymbol{u}_\tau^{(s)}$ into the solution for $\boldsymbol{V}_\tau^{(s)}$, and otherwise does not change the analysis.

The dimensionless velocity $\boldsymbol{u}_\tau^{(s)}$ is represented in (2.42) in the same scale as $\boldsymbol{V}_\tau^{(s)}$ (or $\boldsymbol{v}_\tau^{(s)}$ for that matter). However, as an extraneous factor, it need not be $O(1)$ in this scaling in the same way as the intrinsic inner streaming is. One just needs to assume that $\boldsymbol{u}_\tau^{(s)}$ is not too large, namely $\boldsymbol{u}_\tau^{(s)} = o(\varepsilon^{-2})$, so that the present treatment of the primary oscillatory flow is still valid for leading order. An example when $\boldsymbol{u}_\tau^{(s)} = O(\varepsilon^{-2})$ is considered by Rednikov *et al.* (2003).

As an example of $\boldsymbol{u}_\tau^{(s)} \neq \boldsymbol{0}$, let us mention a rigid sphere steadily rotating under the action of the acoustic field (Rednikov *et al.* 2003). Alternatively, if the boundary in question is a gas–liquid interface (with the present consideration pertaining to the gas phase), there may develop a significant acoustically-induced steady circulation in the liquid phase (Zhao *et al.* 1999*a*; Rednikov *et al.* 2003). We note that, due to the extreme gas-to-liquid property ratios, a gas–liquid interface may still behave as a rigid body with respect to primary oscillations (the acoustic wave) originating in the gas,

with (2.29) holding. But with respect to a steady motion, its 'liquidity' may become apparent.

2.7. *Linearized constitutive relations*

We write

$$\mathrm{d}\rho^* = \left(\frac{\partial\rho^*}{\partial P^*}\right)_{S^*} \mathrm{d}P^* + \left(\frac{\partial\rho^*}{\partial S^*}\right)_{P^*} \mathrm{d}S^*, \tag{2.43}$$

$$\left(\frac{\partial\rho^*}{\partial P^*}\right)_{S^*} = \frac{1}{c^{*2}}, \quad \left(\frac{\partial\rho^*}{\partial S^*}\right)_{P^*} = \left(\frac{\partial\rho^*}{\partial T^*}\right)_{P^*}\left(\frac{\partial T^*}{\partial S^*}\right)_{P^*} = -\frac{\rho^*\beta^* T^*}{c_p^*}, \tag{2.44}$$

$$\mathrm{d}S^* = -\frac{\beta^*}{\rho^*}\mathrm{d}P^* + \frac{c_p^*}{T^*}\mathrm{d}T^*. \tag{2.45}$$

Thus,

$$\mathrm{d}\rho^* = \frac{1}{c^{*2}}\mathrm{d}P^* - \frac{\beta^{*2}T^*}{c_p^*}\left(\frac{c_p^*\rho^*}{\beta^* T^*}\mathrm{d}T^* - \mathrm{d}P^*\right). \tag{2.46}$$

Similarly, for the dynamic viscosity, we have

$$\mathrm{d}\eta^* = \left(\frac{\partial\eta^*}{\partial P^*}\right)_{S^*} \mathrm{d}P^* + \left(\frac{\partial\eta^*}{\partial T^*}\right)_{P^*} \frac{\beta^* T^*}{c_p^*\rho^*}\left(\frac{c_p^*\rho^*}{\beta^* T^*}\mathrm{d}T^* - \mathrm{d}P^*\right), \tag{2.47}$$

where

$$\left(\frac{\partial\eta^*}{\partial P^*}\right)_{S^*} = \left(\frac{\partial\eta^*}{\partial P^*}\right)_{T^*} + \left(\frac{\partial\eta^*}{\partial T^*}\right)_{P^*}\frac{T^*\beta^*}{c_p^*\rho^*}. \tag{2.48}$$

Now using the scales and definitions introduced in § 2.2, (2.46) and (2.47) give rise to the following linearized dimensionless constitutive relations:

$$\mathscr{R} = \mathscr{P} - R_T(\mathscr{T} - \mathscr{P}), \qquad \mathscr{N} = N_S\mathscr{P} - N_T(\mathscr{T} - \mathscr{P}), \tag{2.49}$$

with the dimensionless numbers defined as

$$\left.\begin{aligned} R_T &= \frac{T^*\beta^{*2}c^{*2}}{c_p^*} = \gamma - 1, \quad N_T = -\left(\frac{\partial\eta^*}{\partial T^*}\right)_{P^*}\frac{T^*\beta^* c^{*2}}{c_p^*\eta^*} = -\left(\frac{\partial\eta^*}{\partial T^*}\right)_{P^*}\frac{\gamma-1}{\eta^*\beta^*}, \\ N_S &= \left(\frac{\partial\eta^*}{\partial P^*}\right)_{S^*}\frac{\rho^* c^{*2}}{\eta^*} = \left(\frac{\partial\eta^*}{\partial P^*}\right)_{T^*}\frac{\rho^* c^{*2}}{\eta^*} - N_T, \end{aligned}\right\} \tag{2.50}$$

where $\gamma = c_p^*/c_v^*$, while c_p^* and c_v^* are the specific heats at constant pressure and at constant volume, respectively. All the quantities in (2.50) are evaluated in the unperturbed (background) state of the fluid.

The first and the second terms on the right-hand side of each expression (2.49) correspond to the isentropic and the non-isentropic contributions, respectively. For liquids, $(\gamma - 1)$ is typically small and so the contribution due to R_T must most definitely be negligible. Yet the one due to N_T may still be noticeable (cf. § 3.1) in spite of $(\gamma - 1) \ll 1$.

2.8. *Temperature, density and viscosity fluctuations in the Stokes layer*

In dimensionless form, a linearized boundary-layer version of the heat equation governing the unsteady part of the temperature field in the Stokes layer can be

written as

$$\frac{\partial \mathscr{T}^{(u)}}{\partial t} - \frac{\partial \mathscr{P}^{(u)}}{\partial t} = \frac{1}{Pr}\frac{\partial^2 \mathscr{T}^{(u)}}{\partial Y^2}, \tag{2.51}$$

where

$$Pr = \frac{\nu^*}{\chi^*} \tag{2.52}$$

is the Prandtl number, ν^* is the kinematic viscosity and χ^* is the thermal diffusivity. In terms of the complex amplitudes (2.12), the equation becomes

$$\mathrm{i}(\mathscr{T}^{(u1)} - \mathscr{P}^{(u1)}) = \frac{1}{Pr}\frac{\partial^2 \mathscr{T}^{(u1)}}{\partial Y^2}. \tag{2.53}$$

When the fluid under consideration is a gas (low heat capacity and conductivity), it is reasonable to assume that the temperature fluctuation vanishes at the boundary, i.e.

$$\mathscr{T}^{(u1)} = 0 \qquad \text{at} \quad Y = 0. \tag{2.54}$$

For liquids, this may not be the case. Nonetheless, here we just go through with (2.54), and on a later occasion (§ 3.1) indicate the change in the result in the case of comparable thermal properties of the fluid and the material on the other side of the boundary.

At the outer edge of the Stokes layer, the temperature amplitude approaches its value in the ideal acoustic wave

$$\mathscr{T}^{(u1)} \to p_s^{(u1)} \qquad \text{as} \quad Y \to \infty. \tag{2.55}$$

With (2.32) taken into account, the solution of (2.53)–(2.55) is

$$\mathscr{T}^{(u1)} = p_s^{(u1)}\left\{1 - \mathrm{e}^{-\sqrt{\mathrm{i}}\,Pr^{1/2}Y}\right\}. \tag{2.56}$$

Now, from (2.32), (2.49) and (2.56), we obtain

$$\mathscr{R}^{(u1)} = p_s^{(u1)}\left\{1 + R_T\,\mathrm{e}^{-\sqrt{\mathrm{i}}\,Pr^{1/2}Y}\right\}, \tag{2.57}$$

$$\mathscr{N}^{(u1)} = p_s^{(u1)}\left\{N_S + N_T\,\mathrm{e}^{-\sqrt{\mathrm{i}}\,Pr^{1/2}Y}\right\}. \tag{2.58}$$

2.9. *Primary oscillatory flow in the Stokes layer – part 2*

Finally, we are in a position to complete the solution for the normal velocity. Solving (2.26) with (2.29), (2.33) and (2.57) taken into account, we obtain

$$V_Y^{(u1)} = -\nabla_{\tau s}\cdot \boldsymbol{v}_{\tau s}^{(u1)}\left[Y + \mathrm{i}\sqrt{\mathrm{i}}\{1 - \mathrm{e}^{-\sqrt{\mathrm{i}}\,Y}\}\right] - \mathrm{i}k^2 p_s^{(u1)}\left[Y - \mathrm{i}\sqrt{\mathrm{i}}\frac{R_T}{Pr^{1/2}}\left\{1 - \mathrm{e}^{-\sqrt{\mathrm{i}}\,Pr^{1/2}\,Y}\right\}\right]. \tag{2.59}$$

2.10. *Steady (radiation) pressure and inner streaming*

Now we are set for the calculation of the steady flow component. First, from (2.40), it follows that $\mathscr{P}^{(s)} \neq \mathscr{P}^{(s)}(Y)$. From the matching requirement, it is clear that $p_s^{(s)} = \mathscr{P}^{(s)}$. We proceed from the time-averaged tangential momentum equation in one of the equivalent forms (2.35), (2.38) or (2.39). A result for $\mathscr{P}^{(s)}$ can formally be obtained by requiring the minimal possible singularity in $\boldsymbol{V}_\tau^{(s)}$ as $Y \to \infty$. Thus, requiring no terms $O(Y^2)$ be present in the expression for $\boldsymbol{V}_\tau^{(s)}$ leads to

$$k^2\left\langle p_s^{(u)}\frac{\partial \boldsymbol{v}_{\tau s}^{(u)}}{\partial t}\right\rangle + \frac{1}{2}\nabla_{\tau s}\left\langle \boldsymbol{v}_{\tau s}^{(u)}\cdot \boldsymbol{v}_{\tau s}^{(u)}\right\rangle = -\nabla_{\tau s}\mathscr{P}^{(s)}, \tag{2.60}$$

which follows from (2.35), as well as from the fact that $\boldsymbol{V}_\tau^{(u)} \to \boldsymbol{v}_{\tau s}^{(u)}$ and $\mathscr{P}^{(u)} \to p_s^{(u)}$ as $Y \to \infty$ (cf. (2.33) and (2.57)). As $\partial \boldsymbol{v}_{\tau s}^{(u)}/\partial t = -\nabla_{\tau s} p_s^{(u)}$ (cf. (2.31)), we obtain

$$\mathscr{P}^{(s)} = p_s^{(s)} = -\tfrac{1}{2}\langle \boldsymbol{v}_{\tau s}^{(u)} \cdot \boldsymbol{v}_{\tau s}^{(u)} \rangle + \tfrac{1}{2}k^2 \langle p_s^{(u)2} \rangle = -\tfrac{1}{4}\boldsymbol{v}_{\tau s}^{(u1)} \cdot \overline{\boldsymbol{v}_{\tau s}^{(u1)}} + \tfrac{1}{4}k^2 p_s^{(u1)} \overline{p_s^{(u1)}} \tag{2.61}$$

up to a constant, which is a result for the steady pressure (or, as it is often called, 'radiation pressure') distribution at the boundary.

With (2.33), (2.57)–(2.59) and (2.61), the solution of (2.39), (2.42) is

$$\begin{aligned}
\boldsymbol{V}_\tau^{(s)} = {} & \left[\frac{1}{4}\nabla_{\tau s}\left(\boldsymbol{v}_{\tau s}^{(u1)} \cdot \overline{\boldsymbol{v}_{\tau s}^{(u1)}}\right) + \frac{1}{2}\overline{\boldsymbol{v}_{\tau s}^{(u1)}}\nabla_{\tau s} \cdot \boldsymbol{v}_{\tau s}^{(u1)}\right]\left[\mathrm{i}\mathrm{e}^{-\sqrt{\mathrm{i}}Y} - \mathrm{i}\mathrm{e}^{-\sqrt{-\mathrm{i}}Y} + \frac{1}{2}\mathrm{e}^{-\sqrt{2}Y} - \frac{1}{2}\right] \\
& - \frac{1}{2}\overline{\boldsymbol{v}_{\tau s}^{(u1)}}\nabla_{\tau s} \cdot \boldsymbol{v}_{\tau s}^{(u1)}\left[\mathrm{i}\mathrm{e}^{-\sqrt{\mathrm{i}}Y} + \frac{1+\mathrm{i}}{\sqrt{2}}Y\mathrm{e}^{-\sqrt{-\mathrm{i}}Y} + (\mathrm{i}-1)\,\mathrm{e}^{-\sqrt{-\mathrm{i}}Y} + \frac{1-\mathrm{i}}{2}\mathrm{e}^{-\sqrt{2}Y} + \frac{1-3\mathrm{i}}{2}\right] \\
& - \frac{1}{2}\mathrm{i}k^2\, p_s^{(u1)}\,\overline{\boldsymbol{v}_{\tau s}^{(u1)}}\left[-\mathrm{i}\frac{R_T}{Pr}\,\mathrm{e}^{-\sqrt{\mathrm{i}}Pr^{1/2}Y} + \frac{1+\mathrm{i}}{\sqrt{2}}\,Y\,\mathrm{e}^{-\sqrt{-\mathrm{i}}Y}\right. \\
& + \left(\mathrm{i} + \frac{R_T}{Pr^{1/2}} + \mathrm{i}\,N_S\right)\mathrm{e}^{-\sqrt{-\mathrm{i}}Y} + \left(\mathrm{i}\frac{R_T}{Pr^{1/2}} + N_T\right)\frac{Pr^{1/2}+\mathrm{i}}{1+Pr}\,\mathrm{e}^{-(\sqrt{\mathrm{i}}Pr^{1/2}+\sqrt{-\mathrm{i}})Y} \\
& \left. - \mathrm{i} - \mathrm{i}\,N_S - (R_T + N_T)\frac{Pr^{1/2}}{1+Pr} + \mathrm{i}\left(\frac{R_T}{Pr} - N_T\right)\frac{1}{1+Pr}\right] + \boldsymbol{d}_\tau^{(s)}\,Y + \boldsymbol{u}_\tau^{(s)}.
\end{aligned} \tag{2.62}$$

Here $\sqrt{\pm\mathrm{i}} = (1 \pm \mathrm{i})/\sqrt{2}$. On the right-hand side of (2.62), only the real part is meant. The quantity $\boldsymbol{d}_\tau^{(s)}$ is an arbitrary steady tangential surface vector field (independent of Y). But for the last two terms ($\boldsymbol{d}_\tau^{(s)}\,Y + \boldsymbol{u}_\tau^{(s)}$), (2.62) describes what can be referred to as the *intrinsic* inner streaming. As for $\boldsymbol{d}_\tau^{(s)}$ and $\boldsymbol{u}_\tau^{(s)}$, if non-zero, they owe themselves to extrinsic influences, which in principle may be either eventually related to outer streaming (cf. § 2.11) or rather imposed by unrelated factors (external flows, motion of the boundary).

2.11. *Effective slip velocity and time-averaged tangential stress*

In accordance with (2.11), we have

$$\langle \boldsymbol{v} \rangle = \varepsilon\, \boldsymbol{v}^{(s)}, \tag{2.63}$$

for the steady velocity field in the main bulk of the fluid (the outer steaming). The condition of matching with the steady tangential velocity field (2.62) in the Stokes layer yields

$$\boldsymbol{v}_{\tau s}^{(s)} = \boldsymbol{u}_\tau^{(s)} + \Delta \boldsymbol{v}_{\tau s}^{(s)}, \tag{2.64}$$

and (recall (2.21))

$$\boldsymbol{d}_\tau^{(s)} = \frac{1}{M}\left.\frac{\partial \boldsymbol{v}_\tau^{(s)}}{\partial y}\right|_s, \tag{2.65}$$

where, as usual, the subscript 's' refers to the evaluation at the boundary itself. The quantity $\Delta \boldsymbol{v}_{\tau s}^{(s)}$ is the difference between the values of the intrinsic part of (2.62) at $Y \to \infty$ and $Y = 0$. Namely,

$$\begin{aligned}
\Delta \boldsymbol{v}_{\tau s}^{(s)} = {} & -\frac{1}{8}\nabla_{\tau s}\left(\boldsymbol{v}_{\tau s}^{(u1)} \cdot \overline{\boldsymbol{v}_{\tau s}^{(u1)}}\right) - \frac{1}{4}\mathrm{Re}\left\{(2-3\mathrm{i})\overline{\boldsymbol{v}_{\tau s}^{(u1)}}\nabla_{\tau s} \cdot \boldsymbol{v}_{\tau s}^{(u1)}\right\} + \frac{1}{2}k^2\mathrm{Re}\left\{\mathrm{i}p_s^{(u1)}\overline{\boldsymbol{v}_{\tau s}^{(u1)}}\right. \\
& \left. \times \left[\mathrm{i} + \mathrm{i}N_S + (R_T + N_T)\frac{Pr^{1/2}}{1+Pr} + \mathrm{i}\left(N_T - \frac{R_T}{Pr}\right)\frac{1}{1+Pr}\right]\right\}.
\end{aligned} \tag{2.66}$$

It is referred to as the effective slip velocity in accordance with its appearance in (2.64), which should be regarded as a boundary condition for the outer steady flow. For a motionless rigid boundary, when $\boldsymbol{u}_\tau^{(s)} = \boldsymbol{0}$, $\Delta\boldsymbol{v}_{\tau s}^{(s)}$ may just be the only factor to cause a steady flow in the main bulk (by means of the boundary condition (2.64)). When it is so, we have a pure form of the type II streaming (cf. § 1).

The appearance of an asymptotically large parameter M in (2.65) can mean one of the following. In the case when the outer steady streaming is of the same order of magnitude as the intrinsic inner streaming (that is, if $\boldsymbol{v}^{(s)} = O(1)$, and incidentally such is the case when the outer streaming is caused exclusively by the effective slip velocity), it should be $\boldsymbol{d}_\tau^{(s)} \ll 1$ and the term with $\boldsymbol{d}_\tau^{(s)}$ should be neglected in (2.62). On the other hand, should it happen that $\boldsymbol{d}_\tau^{(s)} = O(1)$, this would necessarily imply $\boldsymbol{v}^{(s)} \gg 1$ ($\langle \boldsymbol{v} \rangle \gg \varepsilon$). In other words, the outer steady flow is asymptotically much more intense than the intrinsic inner streaming. Such an outer flow cannot be caused by just the effective slip velocity. An example where $\boldsymbol{d}_\tau^{(s)} = O(1)$ is actually considered by Rednikov *et al.* (2003). In that example, a steady flow with $\boldsymbol{v}^{(s)} = O(M) \gg 1$ occurs due to the acoustically-induced rotation of a sphere, yielding formally $\boldsymbol{u}_\tau^{(s)} = O(M) \gg 1$ in the present terms. See also the case of a sphere free to rotate in § 3.4.

We note that the normal velocity associated with the intrinsic inner streaming is asymptotically much smaller than the tangential one (cf. (2.22)). Thus, with the same precision as the result (2.64) is written, any jump in the normal velocity across the Stokes layer is negligible, and the counterpart of (2.64) for the normal velocity is merely

$$v_{ns}^{(s)} = u_n^{(s)}, \tag{2.67}$$

where $u_n^{(s)}$ is the steady normal velocity of the boundary in the same scaling as $\boldsymbol{u}_\tau^{(s)}$.

An important characteristic is the steady tangential stress exerted upon the boundary due to the intrinsic inner streaming. Here it is referred to as the induced tangential stress. It is given by

$$\Delta\boldsymbol{\sigma}_{\tau s}^{(s)} = \left.\frac{\partial \boldsymbol{V}_\tau^{(s)}}{\partial Y}\right|_{Y=0,\ \boldsymbol{d}_\tau^{(s)} \equiv \boldsymbol{0}} + \left\langle \mathscr{N}^{(u)} \frac{\partial \boldsymbol{V}_\tau^{(u)}}{\partial Y} \right\rangle \Bigg|_{Y=0}, \tag{2.68}$$

where

$$\left\langle \mathscr{N}^{(u)} \frac{\partial \boldsymbol{V}_\tau^{(u)}}{\partial Y} \right\rangle = \frac{1}{2}\mathrm{Re}\left\{ \mathscr{N}^{(u1)} \frac{\partial \overline{\boldsymbol{V}_\tau^{(u1)}}}{\partial Y} \right\}. \tag{2.69}$$

Taking (2.33), (2.58) and (2.62) into account, (2.68) becomes

$$\Delta\boldsymbol{\sigma}_{\tau s}^{(s)} = \frac{1}{8}\sqrt{2}\,\nabla_{\tau s}\left(\boldsymbol{v}_{\tau s}^{(u1)} \cdot \overline{\boldsymbol{v}_{\tau s}^{(u1)}}\right) + \frac{1}{4}\sqrt{2}\,\mathrm{Re}\left\{\mathrm{i}\overline{\boldsymbol{v}_{\tau s}^{(u1)}}\,\nabla_{\tau s} \cdot \boldsymbol{v}_{\tau s}^{(u1)}\right\} + \frac{1}{4}\sqrt{2}\,k^2\,\frac{R_T}{Pr^{1/2}}\,\mathrm{Re}\left\{(1+\mathrm{i})\,p_s^{(u1)}\,\overline{\boldsymbol{v}_{\tau s}^{(u1)}}\right\}. \tag{2.70}$$

Let us also mention that (2.70) can be obtained directly from (2.39) by integrating the latter from $Y = 0$ to $Y = \infty$, using (2.61) and assuming that $\partial \boldsymbol{V}_\tau^{(s)}/\partial Y \to \boldsymbol{0}$ as $Y \to \infty$.

2.12. *Discussion, practical summary and the incompressible case*

The effective slip velocity $\Delta\boldsymbol{v}_{\tau s}^{(s)}$ and the induced tangential stress $\Delta\boldsymbol{\sigma}_{\tau s}^{(s)}$ constitute the most important information needed about the inner streaming at a motionless boundary. Correspondingly, (2.66) and (2.70) with dimensionless numbers defined in (2.1) and (2.50) are the principal results of the present section, where the steady characteristics (superscript '(s)', understood in the sense (2.11)) are expressed via the

complex amplitudes (superscript '$(u1)$', understood in the sense (2.12), and with the overbar denoting the complex conjugate) of the ideal time-harmonic acoustic field (here in terms of the velocity $\boldsymbol{v}$ and pressure p) evaluated at the boundary in question (subscript 's'). In fact, in view of (2.31), the results (2.66) and (2.70) can be expressed by means of the distribution of a single scalar complex-valued quantity (e.g. $p_s^{(u1)}$) along the boundary. For the sake of a practical summary, let us also recall that the double subscript 'τs' refers to tangential vectors on the boundary (e.g. $\Delta\boldsymbol{v}_{\tau s}^{(s)}$ and $\Delta\boldsymbol{\sigma}_{\tau s}^{(s)}$ are not defined beyond the boundary), or else to tangential projections of three-dimensional vectors (including the gradient operator ∇) evaluated at the boundary (e.g. $\boldsymbol{v}^{(u1)}$ and ∇ yielding $\boldsymbol{v}_{\tau s}^{(u1)}$ and $\nabla_{\tau s}$, respectively). The symbol 'Δ' is used within the notations here to convey the idea of an effective jump, due to the Stokes-layer sheet, in the corresponding quantities as observed on the scale of the main bulk of the fluid. This is clearly seen, e.g. in (2.64), where $\Delta\boldsymbol{v}_{\tau s}^{(s)}$ is the difference between the tangential component of the outer-streaming velocity field at the boundary and the steady tangential velocity of the boundary itself. Let us remember though that, within the same order of approximation, there is no such a jump for the normal velocity (cf. (2.67)), which can symbolically be expressed as $\Delta v_{ns}^{(s)} = 0$. We also note that the dimensional values of the effective slip velocity and the induced tangential stress are (see conventions in §§ 2.2 and 2.3)

$$\langle \Delta\boldsymbol{v}_{\tau s}^{*} \rangle = \varepsilon U^{*} \Delta\boldsymbol{v}_{\tau s}^{(s)}, \quad \langle \Delta\boldsymbol{\sigma}_{\tau s}^{*} \rangle = \frac{\rho^{*} U^{*2}}{M} \Delta\boldsymbol{\sigma}_{\tau s}^{(s)}, \tag{2.71}$$

where we recall that all length and velocity variables are made dimensionless using the scales l^{*} and U^{*}, respectively, that are left free/unspecified in the developments, whereas the pressure is non-dimensionalized with the scale $\rho^{*}\omega^{*}U^{*}l^{*}$. The key dimensionless parameters ε and M are defined in (2.2).

The terms $O(k^2)$ in (2.66) and (2.70) are genuinely related to compressibility and viscosity variability. They come from density and viscosity fluctuations in the Stokes layer. The incompressible limit corresponds to $k \to 0$, and the effect of viscosity variability also vanishes in this limit. Therefore, in the *incompressible* case, we have

$$\Delta\boldsymbol{v}_{\tau s}^{(s)} = -\tfrac{1}{8}\nabla_{\tau s}\left(\boldsymbol{v}_{\tau s}^{(u1)} \cdot \overline{\boldsymbol{v}_{\tau s}^{(u1)}}\right) - \tfrac{1}{4}\mathrm{Re}\left\{(2-3\mathrm{i})\overline{\boldsymbol{v}_{\tau s}^{(u1)}}\nabla_{\tau s} \cdot \boldsymbol{v}_{\tau s}^{(u1)}\right\}, \tag{2.72}$$

$$\Delta\boldsymbol{\sigma}_{\tau s}^{(s)} = \tfrac{1}{8}\sqrt{2}\nabla_{\tau s}\left(\boldsymbol{v}_{\tau s}^{(u1)} \cdot \overline{\boldsymbol{v}_{\tau s}^{(u1)}}\right) + \tfrac{1}{4}\sqrt{2}\mathrm{Re}\left\{\mathrm{i}\overline{\boldsymbol{v}_{\tau s}^{(u1)}}\nabla_{\tau s} \cdot \boldsymbol{v}_{\tau s}^{(u1)}\right\}. \tag{2.73}$$

Thus, within the general results (2.66) and (2.70), one can distinguish an incompressible contribution, as well as contributions due to compressibility and viscosity variability. Furthermore, each of the latter two consists of the adiabatic and the non-adiabatic parts. Thus, five contributions in total can be seen in the result for the effective slip velocity (2.66). Apart from the incompressible contribution, there are the ones associated with the adiabatic effects of compressibility (the term containing no dimensionless number within the square brackets) and viscosity variability (the term with N_S), as well as with the non-adiabatic effects of compressibility (the terms with R_T) and viscosity variability (the terms with N_T). Within the result for the induced tangential stress (2.70), the only non-vanishing contribution, apart from the incompressible one, is the one due to the non-adiabatic effect of compressibility.

2.13. *Component-wise presentation and planar/axisymmetric cases*

To write (2.66) and (2.70) in a component form, an orthogonal curvilinear coordinate system $\{\xi, \eta\}$ is introduced on the boundary. Let $\boldsymbol{e}_{\xi}$ and $\boldsymbol{e}_{\eta}$ be the corresponding unit

vectors ($\boldsymbol{e}_\xi \cdot \boldsymbol{e}_\eta = 0$), while H_ξ and H_η are the corresponding metric coefficients. Then

$$\left.\begin{gathered}\boldsymbol{v}_{\tau s}^{(u1)} = v_{\xi s}^{(u1)}\boldsymbol{e}_\xi + v_{\eta s}^{(u1)}\boldsymbol{e}_\eta, \quad \Delta\boldsymbol{v}_{\tau s}^{(s)} = \Delta v_{\xi s}^{(s)}\boldsymbol{e}_\xi + \Delta v_{\eta s}^{(s)}\boldsymbol{e}_\eta, \quad \Delta\boldsymbol{\sigma}_{\tau s}^{(s)} = \Delta\sigma_{\xi s}^{(s)}\boldsymbol{e}_\xi + \Delta\sigma_{\eta s}^{(s)}\boldsymbol{e}_\eta, \\ \nabla_{\tau s} = \frac{\boldsymbol{e}_\xi}{H_\xi}\frac{\partial}{\partial\xi} + \frac{\boldsymbol{e}_\eta}{H_\eta}\frac{\partial}{\partial\eta}, \quad \nabla_{\tau s}\cdot\boldsymbol{v}_{\tau s}^{(u1)} = \frac{1}{H_\xi H_\eta}\frac{\partial}{\partial\xi}\left(H_\eta v_{\xi s}^{(u1)}\right) + \frac{1}{H_\xi H_\eta}\frac{\partial}{\partial\eta}\left(H_\xi v_{\eta s}^{(u1)}\right).\end{gathered}\right\} \tag{2.74}$$

Now if (2.74) is used in (2.66) and (2.70), and the results are projected in turn on $\boldsymbol{e}_\xi$ and $\boldsymbol{e}_\eta$, we obtain expressions for the components $\Delta v_{\xi s}^{(s)}$, $\Delta v_{\eta s}^{(s)}$, $\Delta\sigma_{\xi s}^{(s)}$ and $\Delta\sigma_{\eta s}^{(s)}$ in terms of the complex amplitudes $v_{\xi s}^{(u1)}$, $v_{\eta s}^{(u1)}$ and $p_s^{(u1)}$. This is the sought component-wise presentation.

Important particular cases are the planar and the axisymmetric ones, and we next accommodate the results (2.66) and (2.70) to these two cases. Let ξ be the significant coordinate. Then no scalar property depends on η and the corresponding vector components are equal to zero. We have $H_\eta = 1$ in the planar case, and $H_\eta = \varrho$ in the axisymmetric one, where ϱ is the dimensionless distance to the symmetry axis (the cylindrical radius). Using all this in (2.74) and then in (2.66) and (2.70), we obtain

$$\begin{aligned}\Delta v_{\xi s}^{(s)} = {} & -\frac{3}{8H_\xi}\frac{\partial}{\partial\xi}\left|v_{\xi s}^{(u1)}\right|^2 + \frac{3}{4H_\xi}\mathrm{Re}\left\{\mathrm{i}\overline{v_{\xi s}^{(u1)}}\frac{\partial v_{\xi s}^{(u1)}}{\partial\xi}\right\} - \frac{n}{2H_\xi\varrho}\frac{\partial\varrho}{\partial\xi}\left|v_{\xi s}^{(u1)}\right|^2 \\ & + \frac{1}{2}k^2\mathrm{Re}\left\{\mathrm{i}p_s^{(u1)}\overline{v_{\xi s}^{(u1)}}\left[\mathrm{i} + \mathrm{i}N_S + (R_T + N_T)\frac{Pr^{1/2}}{1+Pr} + \mathrm{i}\left(N_T - \frac{R_T}{Pr}\right)\frac{1}{1+Pr}\right]\right\}\end{aligned} \tag{2.75}$$

with

$$n = \begin{cases} 0, & \text{planar case,} \\ 1, & \text{axisymmetric case,} \end{cases} \tag{2.76}$$

and

$$\begin{aligned}\Delta\sigma_{\xi s}^{(s)} = {} & \frac{1}{4\sqrt{2}H_\xi}\frac{\partial}{\partial\xi}\left|v_{\xi s}^{(u1)}\right|^2 + \frac{1}{2\sqrt{2}H_\xi}\mathrm{Re}\left\{\mathrm{i}\overline{v_{\xi s}^{(u1)}}\frac{\partial}{\partial\xi}v_{\xi s}^{(u1)}\right\} \\ & + \frac{1}{4}\sqrt{2}k^2\frac{R_T}{Pr^{1/2}}\mathrm{Re}\left\{(1+\mathrm{i})p_s^{(u1)}\overline{v_{\xi s}^{(u1)}}\right\}\end{aligned} \tag{2.77}$$

for both cases.

3. Examples

3.1. *Standing wave grazing a parallel wall: estimation of the non-adiabatic effects*

This is a classical problem of acoustic streaming. We have a one-dimensional acoustic standing wave along the z-axis, and a flat rigid wall parallel to it. The primary oscillatory flow is given by

$$\varphi^{(u1)} = \frac{1}{k}\sin kz, \tag{3.1}$$

in terms of the complex amplitude of the velocity potential, $\boldsymbol{v}^{(u1)} = \nabla\varphi^{(u1)}$.

Here the velocity amplitude of the wave is chosen as the velocity scale U^* (cf. § 2.2). Without loss of generality, the length scale l^* can be specified such that e.g. $k \equiv 1$, or $k \equiv 2\pi$. However, we prefer to keep 'k' in the expressions, and accordingly we let l^* be a free parameter. In order to calculate the effective slip velocity at the wall,

(2.75) is used. With (3.1), the quantities to be substituted into (2.75) are obviously the following:

$$n = 0, \quad \xi \equiv z, \quad H_z = 1, \quad v_{zs}^{(u1)} = \cos kz, \quad p_s^{(u1)} = -\mathrm{i}\varphi_s^{u1} = -\mathrm{i}k^{-1}\sin kz. \tag{3.2}$$

One finally obtains

$$\Delta v_{zs}^{(s)} = \left(\tfrac{3}{8} + \tfrac{1}{4}B_T\right)k\sin 2kz \tag{3.3}$$

with

$$B_T \equiv (R_T + N_T)\frac{Pr^{1/2}}{1+Pr}. \tag{3.4}$$

Apart from the classical factor 3/8, we find an additional contribution due to the non-adiabatic effects of compressibility and variable viscosity. Such a contribution is often ignored in the literature. Interestingly enough, in the case when the leading-order primary oscillatory flow is all in phase (as in the standing wave here), both effects enter the result for the effective slip velocity by means of one single combination (3.4). As seen from (2.66), this is a general feature, which is not limited to the present geometry of the standing wave. On the other hand, it is also a general feature in such circumstances that the *adiabatic* effects of compressibility and variable viscosity do not contribute at all. This explains why the correct factor 3/8 (in terms of (3.3)) can be obtained by formally treating the Stokes layer as incompressible (e.g. as done in the book of Landau & Lifshitz 1988).

For gases, the coefficient of viscosity typically grows with temperature. Therefore, as seen from (2.50) and (3.4), the effect of variable viscosity acts in the opposite way to the one of compressibility, thus reducing the overall non-adiabatic effect in the effective slip velocity (3.3) rather than reinforcing it. For estimation, we take $Pr^{1/2}/(1+Pr) \approx 1/2$ for gases. For monatomic ideal gases, we have $R_T = \gamma - 1 = 2/3$. For diatomic gases, $R_T = 2/5$. Besides, if the dynamic viscosity as a function of the absolute temperature is $\eta^* \sim \sqrt{T^*}$, and $\beta^* = 1/T^*$ as for ideal gases, then (see (2.50)) $N_T = -(1/2)R_T$. Finally, it turns out that $B_T \approx 1/6$ for monatomic ideal gases, and $B_T \approx 1/10$ for diatomic ideal gases. Within (3.3), this amounts to +11 % and +7 % alterations upon the factor 3/8, respectively, where the positive sign indicates that the value is increased. Thus, the overall effect is not large, but still noticeable.

In the case of liquids, the value of $R_T = \gamma - 1$ is generally small. Thus, the compressibility effect in (3.3) is typically negligible for liquids. However, it is not that simple with the viscosity variability. Indeed, the dynamic viscosity of liquids may be rather sensitive to temperature, much more so than the density is, so that the factor

$$\left(\frac{\partial\eta^*}{\partial T^*}\right)_{P^*}\frac{1}{\eta^*\beta^*} \tag{3.5}$$

may be quite large to offset a small factor $(\gamma - 1)$ within N_T (see (2.50)). Let us estimate N_T according to (2.50). For water at 20 °C, we have (see e.g. Lide 2003) $\eta^* = 10^{-3}\,\mathrm{kg\,m^{-1}\,s^{-1}}$, $(\partial\eta^*/\partial T^*)_{P^*} = -0.25\times10^{-4}\,\mathrm{kg\,m^{-1}\,s^{-1}\,K^{-1}}$, $\beta^* = 0.21\times10^{-3}\,\mathrm{K^{-1}}$, $Pr = 7.0$, $T^* = 293\,\mathrm{K}$. For water at 30 °C, one has $\eta^* = 0.8\times10^{-3}\,\mathrm{kg\,m^{-1}\,s^{-1}}$, $(\partial\eta^*/\partial T^*)_{P^*} = -0.17\times10^{-4}\,\mathrm{kg\,m^{-1}\,s^{-1}\,K^{-1}}$, $\beta^* = 0.30\times10^{-3}\,\mathrm{K^{-1}}$, $Pr = 5.4$, $T^* = 303\,\mathrm{K}$. Further, we just take $c^* = 1500\,\mathrm{m\,s^{-1}}$ and $c_p^* = 4200\,\mathrm{J\,kg^{-1}}$, neglecting their difference at the two temperatures considered. For 20 °C, one obtains $N_T = 0.82$, $B_T = 0.27$ (assuming that $R_T \approx 0$), and this amounts to a +18 % effect within (3.3). For 30 °C, the numbers are $N_T = 1.03$, $B_T = 0.38$ and +25 %. These turn out to be rather significant contributions, and the result is somewhat surprising. Apparently, for liquids, the values of N_T and B_T can substantially vary depending on the liquid

and the conditions (such as the temperature). Even larger values can in principle be expected for some other liquids, especially taking into account that the thermal expansion coefficient β^* for water happens to be lower than the typical value for liquids. Note though that, concerning the derivation of § 2, it has been assumed that the wall is much more heat-conducting than the fluid. This can be considered to be a valid assumption for gases, but may not be so for liquids. Then, the expression for B_T (3.4) should be modified as

$$B_T \equiv (R_T + N_T)\frac{Pr^{1/2}}{1+Pr}\frac{1}{1+\delta_\kappa \delta_\chi^{-1/2}}, \tag{3.6}$$

where δ_κ and δ_χ are the fluid-to-wall ratios of heat conductivities and thermal diffusivities, respectively. At $\delta_\kappa = 0$, (3.4) is recovered. A finite value of $\delta_\kappa \delta_\chi^{-1/2}$ leads to a reduction of the overall effect. At $\delta_\kappa = \infty$, the wall is insulating, and the non-adiabatic contribution vanishes. In any case, we conclude that, for liquids, the non-adiabatic effect of variable viscosity can potentially lead to a significant contribution into the effective slip velocity (and consequently, the outer streaming induced by the latter). This effect is always worth estimating when dealing with a particular situation at hand.

Using (3.2) in (2.77), one obtains the following result for the induced tangential stress:

$$\Delta\sigma_{zs}^{(s)} = -\frac{1}{8}\sqrt{2}\left(1 - \frac{R_T}{Pr^{1/2}}\right) k \sin 2kz. \tag{3.7}$$

The only non-adiabatic contribution here is due to compressibility, but not viscosity variability. For liquids, the R_T term is most certainly insignificant. For gases, however, it can amount to a considerable contribution, much more so than within the effective slip velocity. Indeed, taking for estimation $Pr = 1$, the effect is $-67\,\%$ for monatomic ideal gases, and $-40\,\%$ for diatomic ideal gases. In view of a minus sign, the result (3.7) is altered even more dramatically than it would be with the same values for a plus sign.

3.2. *Small rigid sphere at an arbitrary position within the standing wave*

Now consider the same standing wave (3.1) and suppose that a small rigid sphere is placed in its way. We will be concerned with the acoustic streaming owing to the presence of the sphere. This can be, for instance, a model for the streaming around a sphere levitated in an acoustic levitator. Here we assume that the sphere is at rest and not engaged in oscillatory motion due to the acoustic wave. This means that either the sphere is fixed or, if freely levitated, its inertia is high as compared with the surrounding fluid (e.g. a solid particle in air). The length scale l^* is now chosen to be the sphere's radius. We assume that the sphere is small as compared with the acoustic wavelength, that is $k \ll 1$, and construct the solution as an expansion in terms of k retaining a few first terms.

Let $z = z_0$ be the location of the centre of the sphere. The velocity antinode (pressure node) corresponds to $\sin kz_0 = 0$, while the velocity node (pressure antinode) to $\cos kz_0 = 0$. The problem is axisymmetric. The consideration is carried out in the spherical coordinates $\{r, \theta\}$ such that

$$z - z_0 = r\cos\theta, \tag{3.8}$$

while $r = 1$ corresponds to the surface of the sphere.

The complex amplitude of the potential, $\varphi^{(u1)}$, satisfies the Helmholtz equation

$$(\nabla^2 + k^2)\varphi^{(u1)} = 0 \tag{3.9}$$

and the zero-normal-velocity condition at the surface of the sphere

$$\frac{\partial \varphi^{(u1)}}{\partial r} = 0 \quad \text{at } r = 1. \tag{3.10}$$

If we are interested in the first few terms of the solution in the region $r = O(1)$, the following boundary condition is applicable:

$$\varphi^{(u1)} \to k^{-1}\sin kz_0 + \cos kz_0 r\cos\theta - \tfrac{1}{2}k\sin kz_0 r^2\cos^2\theta + O(k^2) \text{ as } r \to \infty, \tag{3.11}$$

with the right-hand side being (*up to the order considered*) merely an expansion of (3.1) with k, where (3.8) is taken into account.

The solution of (3.9)–(3.11) is

$$\varphi^{(u1)} = \sin kz_0\left(k^{-1} - \frac{1}{6}kr^2 - \frac{k}{3r}\right) + \cos kz_0\left(r + \frac{1}{2r^2}\right)\cos\theta - \frac{1}{6}k\sin kz_0\left(r^2 + \frac{2}{3r^3}\right)(3\cos^2\theta - 1) + O(k^2). \tag{3.12}$$

Now the complex amplitudes of the tangential velocity and pressure at the surface of the sphere are

$$\left.\begin{aligned} v_{\theta s}^{(u1)} &= \left.\frac{\partial\varphi^{(u1)}}{\partial\theta}\right|_{r=1} = -\frac{3}{2}\cos kz_0\sin\theta + \frac{5}{3}k\sin kz_0\sin\theta\cos\theta + O(k^2), \\ p_s^{(u1)} &= -\mathrm{i}\varphi^{(u1)}\big|_{r=1} = -\mathrm{i}k^{-1}\sin kz_0 + O(k^0), \end{aligned}\right\} \tag{3.13}$$

and these are to be used in (2.75) together with

$$n = 1, \quad \xi \equiv \theta, \quad H_\theta = 1, \quad \varrho = \sin\theta, \tag{3.14}$$

in order to calculate the effective slip velocity

$$\Delta v_{\theta s}^{(s)} = -\tfrac{45}{16}\cos^2 kz_0\sin\theta\cos\theta + \tfrac{5}{8}k\sin kz_0\cos kz_0\sin\theta\left(13\cos^2\theta - 3 - \tfrac{6}{5}B_T\right) - \tfrac{25}{36}k^2\sin^2 kz_0\sin\theta\cos\theta\left(8\cos^2\theta - 3 - \tfrac{6}{5}B_T\right) + O(k^2\cos^2 kz_0; k^3), \tag{3.15}$$

where the definition (3.4) has been used.

In view of the axial symmetry, it is convenient to consider the outer steady streaming in terms of the stream function

$$v_r^{(s)} = \frac{1}{r^2\sin\theta}\frac{\partial\psi^{(s)}}{\partial\theta}, \quad v_\theta^{(s)} = -\frac{1}{r\sin\theta}\frac{\partial\psi^{(s)}}{\partial r}. \tag{3.16}$$

The surface boundary conditions are

$$\psi^{(s)} = 0, \quad \frac{\partial\psi^{(s)}}{\partial r} = -\sin\theta\,\Delta v_{\theta s}^{(s)} \qquad \text{at} \quad r = 1. \tag{3.17}$$

Since the streaming is expected to fade away far off the sphere,

$$\psi^{(s)}/r^2 \to 0 \qquad \text{as} \quad r \to \infty. \tag{3.18}$$

Here we limit ourselves to the case of small streaming Reynolds numbers,

$$\varepsilon U^* l^*/\nu^* = \varepsilon^2 M^2 \ll 1. \tag{3.19}$$

We note that a similar large-Reynolds-number problem with the same kind of distribution of the effective slip velocity is treated in Amin & Riley (1990). Then $\psi^{(s)}$ satisfies the Stokes equation

$$E^2E^2\psi^{(s)} = 0, \qquad E^2 = \frac{\partial^2}{\partial r^2} + \frac{\sin^2\theta}{r^2}\frac{\partial^2}{\partial\theta^2}, \tag{3.20}$$

(see Happel & Brenner 1965, for the general solution of (3.20)). The solution of the problem (3.17), (3.18), (3.20) with (3.15) taken into account is

$$\begin{aligned}\psi^{(s)} = {} & \frac{45}{32}\cos^2 kz_0\left(1-\frac{1}{r^2}\right)\cos\theta\sin^2\theta + k\sin kz_0\cos kz_0\left\{\frac{1}{8}(1+3B_T)\left(r-\frac{1}{r}\right)\right. \\ & \left. - \frac{13}{16}\left(\frac{1}{r}-\frac{1}{r^3}\right)(5\cos^2\theta-1)\right\}\sin^2\theta + k^2\sin^2 kz_0\left\{\left(\frac{25}{168}-\frac{5}{12}B_T\right)\left(1-\frac{1}{r^2}\right)\right. \\ & \left. + \frac{25}{63}\left(\frac{1}{r^2}-\frac{1}{r^4}\right)(7\cos^2\theta-3)\right\}\cos\theta\sin^2\theta + O(k^2\cos^2 kz_0; k^3).\end{aligned} \tag{3.21}$$

There is a rationale for keeping the $O(k^2\sin^2 kz_0)$ term in (3.15) and (3.21) even though the $O(k^2\cos^2 kz_0)$ term is neglected. Here we are not interested in corrections as such, but rather in obtaining a solution uniformly valid for *all* positions of the sphere in the standing wave. The term $O(k^2\sin^2 kz_0)$ is essential to this goal as the leading-order one at the velocity node (at which $\cos kz_0 = 0$ and $\sin^2 kz_0 = 1$), whereas $O(k^2\cos^2 kz_0)$ is always just a correction. Thus, as written, (3.15) and (3.21) yield such a uniformly valid result. (Note though that an acoustically levitated rigid sphere is normally located below the velocity antinode, but above the halfway between the antinode and the next lowest node. To bring it closer to the node, and in particular at the node itself, the sphere needs to be forcefully positioned there.)

A few words concerning the decay of the outer streaming (3.21) far away from the sphere ($r \to \infty$). One can see that, in terms of the velocity field, it decays as $O(r^{-2})$ when the sphere is either at the velocity antinode or at the velocity node. On the other hand, the decay is slower, $O(r^{-1})$, for the intermediate positions of the sphere. The latter is due to the so-called stokeslet term (cf. Happel & Brenner 1965), which signals to a non-zero net force exerted by the streaming upon the sphere when displaced from the antinode or the node. Note though that this is nothing more than just a correction to the force, the leading-order term being actually due to the radiation pressure (2.61).

With the substitutions

$$\psi^{(s)\prime} \equiv \psi^{(s)}/(\cos^2 kz_0 + k^2\sin^2 kz_0), \tag{3.22}$$

$$K \equiv -k\tan kz_0, \tag{3.23}$$

(3.21) can be rewritten as

$$\begin{aligned}\psi^{(s)\prime} = {} & \frac{45}{32}\frac{1}{1+K^2}\left(1-\frac{1}{r^2}\right)\cos\theta\sin^2\theta + \frac{K}{1+K^2}\left\{-\frac{1}{8}(1+3B_T)\left(r-\frac{1}{r}\right)\right. \\ & \left. + \frac{13}{16}\left(\frac{1}{r}-\frac{1}{r^3}\right)(5\cos^2\theta-1)\right\}\sin^2\theta + \frac{K^2}{1+K^2}\left\{\left(\frac{25}{168}-\frac{5}{12}B_T\right)\left(1-\frac{1}{r^2}\right)\right. \\ & \left. + \frac{25}{63}\left(\frac{1}{r^2}-\frac{1}{r^4}\right)(7\cos^2\theta-3)\right\}\cos\theta\sin^2\theta,\end{aligned} \tag{3.24}$$

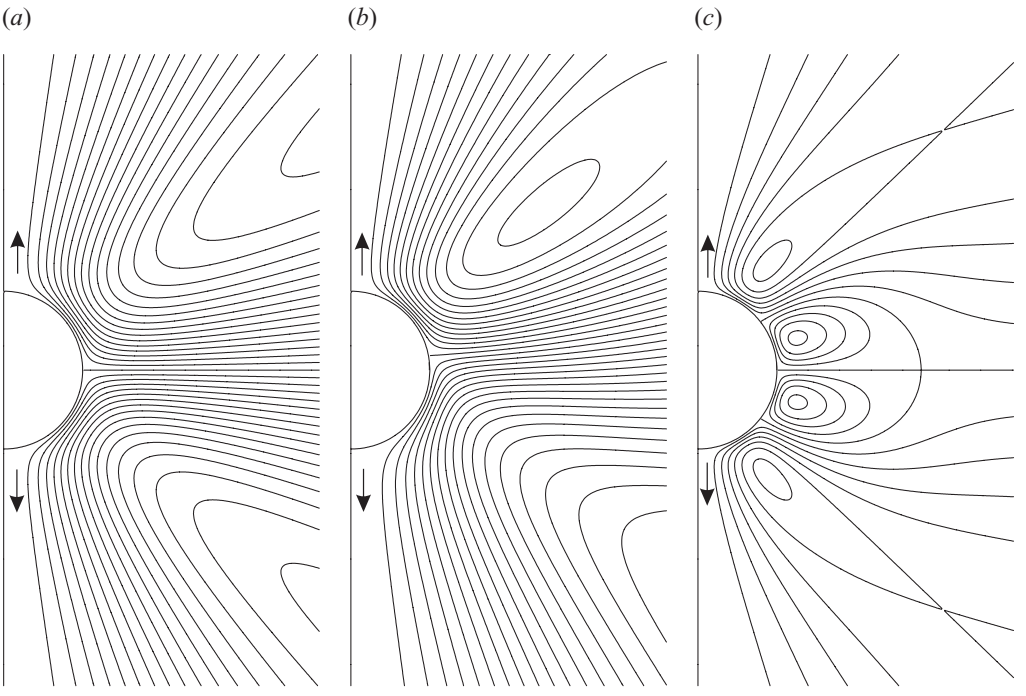

FIGURE 1. Steady streaming from a small rigid sphere placed at various positions within a plane acoustic standing wave (in the Stokes approximation and for $B_T = 0$, see (3.24)). The flow direction is indicated by arrows. (*a*) $K = 0$ (velocity antinode), (*b*) $K = 0.3$ (below the antinode), (*c*) $K = \infty$ (velocity node).

uniformly to leading order. It is remarkable that the flow pattern (3.21) depends on k and z_0 by means of a single combination, K, introduced in (3.23). With the flow intensity factored out with the help of (3.22), this is put into evidence by (3.24). The flow pattern is shown in figure 1 for a number of K values: $K = 0$ (the sphere at the velocity antinode), $K = 0.3$ (the sphere displaced below the antinode, but still above the node; that is supposing that the z-axis points vertically upwards), and $K = \infty$ (the sphere at the velocity node). It has been plotted for $B_T = 0$, although for the cases shown it remains more or less the same for the values of B_T typical for gases (see § 3.1). The first diagram is just the classical result for the steady streaming around a rigid sphere in a uniformly and uniaxially oscillating incompressible fluid medium (Riley 1966). The flow pattern is not only axisymmetric, but also symmetric with respect to the equatorial plane. The second diagram is similar to one of those of Lee & Wang (1990), except that they had the sphere displaced above the antinode ($K < 0$ in our terms), so that their flow pattern appears vertically inverted as compared with ours. At $K = \infty$, when the sphere is at the velocity node, the results of Zhao *et al.* (1999*b*) are recovered. As seen from figure 1(*c*), the velocity field once again becomes symmetric with respect to the equatorial plane when at the velocity node. Similar diagrams have been obtained by Gopinath & Trinh (2000). Note though that, in real acoustic levitators, such a localized streaming from a particle as considered here ('microstreaming') may get distorted by the streaming on a scale of the levitator as a whole, existing even in the absence of the particle, as shown experimentally by Trinh & Robey (1994). For a simple model accounting for this effect, see Rednikov & Riley (2002).

There are a few more comments on the mathematical nature of the result (3.24). First of all, we underscore once again that (3.24) can be viewed as a leading-order (for $k \ll 1$) result uniformly valid for all possible positions of the sphere. Even though (3.24) is valid only for $k \ll 1$, any value of K is admissible there. As seen from (3.23), however small k might be, one can always position the sphere so close to the velocity node that K is finite, or even large. Conversely, K being of order unity or large inevitably (as long as (3.24), as well as (3.21), remains a valid approximation) implies that the sphere is close enough to the velocity node. On the other hand, when the sphere is not close to the velocity node (which is admittedly the main case of interest for acoustically levitated rigid particles), K needs to be small for (3.24) to be a valid approximation. For a small K, (3.24) provides both a valid leading-order result, and a valid $O(K)$ correction. The $O(K^2)$ correction is not a valid one, however, (even though the $O(K^2)$ contribution is perfectly valid for $K = O(1)$), since part of the $O(k^2)$ terms has been ignored in the analysis leading to (3.21) and (3.24). The $O(k^2)$ terms have been calculated in detail in Gopinath & Trinh (2000). Note though that they disregard the effect of variable viscosity. In our analysis, their result corresponds to $N_T \equiv 0$ in (3.4).

Finally, let us mention that a generalization of the result (3.21) up to and including $O(k)$ to the case of a spherical drop whose dynamic viscosity is much greater than that of the external fluid (e.g. a drop in air) was carried out in a recent work by Rednikov *et al.* (2006), albeit in the absence of non-adiabatic effects ($B_T = 0$). Consideration of the internal circulation in the drop was an integral part of the study. In the present paper, an example involving such a liquid sphere is treated in § 3.4.

3.3. *Oblate spheroid vibrating along its axis in an incompressible fluid medium*

Consider now a rigid oblate spheroid performing harmonic high-frequency translational vibrations along its axis relative to an incompressible fluid medium of infinite extent. We work in the reference frame, where the spheroid is at rest and it is the medium far away of it that oscillates. Note that, in the incompressible case, the inner streaming does not depend on whether this frame of reference is inertial or not as long as no rotations are involved, and thus the incompressible results of § 2 are still applicable. Within the set-up of § 3.2 (a particle in an acoustic standing wave), the present consideration corresponds just to the leading order in the small acoustic wavenumber for a spheroid aligned with the direction of the wave and located sufficiently far from the velocity node. The velocity scale U^* is here chosen to coincide with the velocity amplitude of the vibrations, whereas l^* is a linear size of the spheroid (whichever is deemed convenient).

We work in the (modified) oblate spheroidal coordinates $\{\mu, \lambda\}$. If $\{z, \varrho\}$ are the cylindrical coordinates with z being along the symmetry axis and ϱ the radial distance to the axis, then $\{\mu, \lambda\}$ are defined as $z - z_0 = c\lambda\mu$, $\varrho = c\,(1+\lambda^2)^{1/2}(1-\mu^2)^{1/2}$, where c is the dimensionless focal radius and $z = z_0$ corresponds to the centre of the spheroid. The coordinate surfaces defined by constant λ form a family of confocal oblate spheroids. Let $\lambda = \lambda_0$ correspond to the physical oblate spheroid we are considering. Its major (equatorial) and minor (polar) radii are $a = c(1 + \lambda_0^2)^{1/2}$ and $b = c\lambda_0$, and the aspect ratio depends on λ_0 only: $a/b = (1+\lambda_0^2)^{1/2}/\lambda_0$. The value of c is determined by the choice of the length scale l^*. Two reasonable choices for l^* are the major radius (in this case $a \equiv 1$ and $c = (1 + \lambda_0^2)^{-1/2}$), or the equivalent spherical radius ($a^2 b \equiv 1$ and $c = \lambda_0^{-1/3}(1 + \lambda_0^2)^{-1/3}$). The problem for the primary oscillatory flow (in terms of

the complex amplitude of the velocity potential) is

$$\left.\begin{aligned} &\nabla^2\varphi^{(u1)}=0, \quad \nabla^2=\frac{1}{c^2(\lambda^2+\mu^2)}\left\{\frac{\partial}{\partial\lambda}(1+\lambda^2)\frac{\partial}{\partial\lambda}+\frac{\partial}{\partial\mu}(1-\mu^2)\frac{\partial}{\partial\mu}\right\}, \\ &\varphi^{(u1)}\sim c\lambda\mu \quad \text{as } \lambda\to\infty, \qquad \frac{\partial\varphi^{(u1)}}{\partial\lambda}=0 \quad \text{at } \lambda=\lambda_0. \end{aligned}\right\} \tag{3.25}$$

With solutions of the Laplace equation representable as $P_n(\mathrm{i}\lambda)P_n(\mu)$ and $Q_n(\mathrm{i}\lambda)P_n(\mu)$ ($n=0,1,\ldots$ with P and Q being the Legendre functions of the first and second kind, respectively), the solution of our problem can be written as

$$\varphi^{(u1)}=c\left[\lambda-\frac{1+\lambda_0^2}{(1+\lambda_0^2)\operatorname{arccot}(\lambda_0)-\lambda_0}\left(\lambda\operatorname{arccot}(\lambda)-1\right)\right]\mu, \tag{3.26}$$

of which in what follows we shall only need its value at the surface

$$\varphi_s^{(u1)}\equiv\varphi^{(u1)}\big|_{\lambda=\lambda_0}=c\frac{1}{(1+\lambda_0^2)\operatorname{arccot}(\lambda_0)-\lambda_0}\mu. \tag{3.27}$$

In order to calculate the effective slip velocity at the spheroid surface, we use (2.75) with the following values:

$$n=1, \quad k=0, \quad \xi\equiv\mu, \quad H_\mu=\frac{c\left(\lambda_0^2+\mu^2\right)^{1/2}}{(1-\mu^2)^{1/2}}, \quad \varrho=c\left(1+\lambda_0^2\right)^{1/2}(1-\mu^2)^{1/2}, \tag{3.28}$$

together with

$$v_{\mu s}^{(u1)}=\frac{1}{H_\mu}\frac{\partial\varphi_s^{(u1)}}{\partial\mu}, \quad p_s^{(u1)}=-\mathrm{i}\varphi_s^{(u1)} \tag{3.29}$$

and the earlier derived expression for $\varphi_s^{(u1)}$. We finally obtain

$$\Delta v_{\mu s}^{(s)}=\frac{1}{4c\left[\left(1+\lambda_0^2\right)\operatorname{arccot}(\lambda_0)-\lambda_0\right]^2}\left[\frac{3\mu(1-\mu^2)^{3/2}}{\left(\lambda_0^2+\mu^2\right)^{5/2}}+\frac{5\mu(1-\mu^2)^{1/2}}{\left(\lambda_0^2+\mu^2\right)^{3/2}}\right], \tag{3.30}$$

which coincides with the result derived in Rednikov & Sadhal (2004) by means of a direct calculation. Here the use of the developments of §2 has permitted to obtain it with considerably less effort. For further analysis of the present oblate-spheroid problem, including the outer streaming engendered by this distribution of the effective slip velocity, see Rednikov & Sadhal (2004). The present result for the effective slip velocity has also been applied to drops highly flattened by the acoustic field (Lee, Sadhal & Rednikov 2008), where it is deemed to be a satisfactory approximation.

3.4. *Translational three-dimensional oscillation of a sphere in an incompressible fluid medium*

As in § 3.3, here also we consider harmonic high-frequency translational vibrations of a particle relative to an incompressible fluid medium of infinite extent. The particle is simpler than in § 3.3: it is just a sphere. But the oscillation is more complex: it is now a general (three-dimensional, non-uniaxial) translational vibration. In the reference frame where the sphere is at rest, the fluid medium far away uniformly oscillates at a velocity $\boldsymbol{u}_\infty(t)=\mathrm{Re}\{\boldsymbol{u}_\infty^{(u1)}\mathrm{e}^{\mathrm{i}t}\}$, where $\boldsymbol{u}_\infty^{(u1)}$ is a constant complex-valued vector. The velocity scale U^* used here is just a quantity of the order of $|\boldsymbol{u}_\infty^{(u1)*}|$ (we shall not specify it more precisely), whereas l^* is the radius of the sphere.

Any $\boldsymbol{u}_\infty^{(u1)}$ can actually be represented in the form $\boldsymbol{u}_\infty^{(u1)}=[u_{\infty 1}^{(u1)}\boldsymbol{e}_1+u_{\infty 2}^{(u1)}\mathrm{e}^{-\mathrm{i}\pi/2}\boldsymbol{e}_2]\,\mathrm{e}^{\mathrm{i}\psi_0}$, where $\boldsymbol{e}_1$ and $\boldsymbol{e}_2$ are two orthogonal unit vectors ($\boldsymbol{e}_1\cdot\boldsymbol{e}_1=1$, $\boldsymbol{e}_2\cdot\boldsymbol{e}_2=1$, $\boldsymbol{e}_1\cdot\boldsymbol{e}_2=0$),

$u_{\infty 1}^{(u1)} > 0$ and $u_{\infty 2}^{(u1)} > 0$ are positive real values, whereas ψ_0 is a phase (immaterial from the viewpoint of steady streaming). In other words, a general harmonic translational oscillation is representable as a linear combination of two spatially-orthogonal quadrature-phase (phase shift $\pi/2$) uniaxial oscillations. Thus, if imagined as a radius vector, the vector $\boldsymbol{u}_\infty(t)$ just traces an elliptic orbit whose axes are oriented along $\boldsymbol{e}_1$ and $\boldsymbol{e}_2$ (and so do the actual fluid-element trajectories far away from the sphere), the sense of circulation being from $\boldsymbol{e}_1$ towards $\boldsymbol{e}_2$. The following is a useful vector that immediately yields the spatial orientation and the sense of the orbit (by means of the corkscrew rule):

$$\mathrm{Im}\boldsymbol{u}_\infty^{(u1)} \times \mathrm{Re}\boldsymbol{u}_\infty^{(u1)} = \frac{\mathrm{i}}{2}\overline{\boldsymbol{u}_\infty^{(u1)}} \times \boldsymbol{u}_\infty^{(u1)} = u_{\infty 1}^{(u1)} u_{\infty 2}^{(u1)} \boldsymbol{e}_3 \quad \text{with } \boldsymbol{e}_3 \equiv \boldsymbol{e}_1 \times \boldsymbol{e}_2. \tag{3.31}$$

In the particular case of a *uniaxial* oscillation, this vector is equal to zero ($\overline{\boldsymbol{u}_\infty^{(u1)}} \times \boldsymbol{u}_\infty^{(u1)} = \boldsymbol{0}$) and the ellipse degenerates into a line (either $u_{\infty 1}^{(u1)} = 0$ or $u_{\infty 2}^{(u1)} = 0$). This is the case mostly considered (often by default) in the literature. In the opposite particular case ('*circular polarization*'), we have $u_{\infty 1}^{(u1)} = u_{\infty 2}^{(u1)} \equiv u_\infty^{(u1)}$, while a simple criterion in terms of $\boldsymbol{u}_\infty^{(u1)}$ can be written as $\boldsymbol{u}_\infty^{(u1)} \cdot \boldsymbol{u}_\infty^{(u1)} = 0$ (here note that $\boldsymbol{u}_\infty^{(u1)} \cdot \boldsymbol{u}_\infty^{(u1)}$ should not be confused with $|\boldsymbol{u}_\infty^{(u1)}|^2 = \boldsymbol{u}_\infty^{(u1)} \cdot \overline{\boldsymbol{u}_\infty^{(u1)}}$). It is actually the circular-polarization case that is treated by Rednikov *et al.* (2003) for steady streaming from cylinders and spheres.

The (complex amplitude of the) velocity potential of the primary oscillatory flow in the main bulk is given by the problem

$$\nabla^2 \varphi^{(u1)} = 0, \tag{3.32}$$

$$\varphi^{(u1)} \sim r\left(\boldsymbol{u}_\infty^{(u1)} \cdot \boldsymbol{e}_r\right) \quad \text{as } r \to \infty, \qquad \partial\varphi^{(u1)}/\partial r = 0 \quad \text{at } r = 1 \tag{3.33}$$

with the solution

$$\varphi^{(u1)} = \left(r + \frac{1}{2r^2}\right)\left(\boldsymbol{u}_\infty^{(u1)} \cdot \boldsymbol{e}_r\right) \tag{3.34}$$

yielding the following values at the surface ($r = 1$):

$$\varphi_s^{(u1)} = \tfrac{3}{2}\boldsymbol{u}_\infty^{(u1)} \cdot \boldsymbol{e}_r, \quad \boldsymbol{v}_{\tau s}^{(u1)} = \nabla_{\tau s}\varphi_s^{(u1)} = \tfrac{3}{2}\left[\boldsymbol{u}_\infty^{(u1)} - \left(\boldsymbol{u}_\infty^{(u1)} \cdot \boldsymbol{e}_r\right)\boldsymbol{e}_r\right]. \tag{3.35}$$

Here r is the radial coordinate, $\boldsymbol{e}_r$ is the unit vector in the radial direction. Note an important identity $\nabla_{\tau s}\boldsymbol{e}_r = \boldsymbol{I} - \boldsymbol{e}_r\boldsymbol{e}_r$ (in polyadic notations), used in (3.35) and useful in what follows, where $\boldsymbol{I}$ is the identity tensor.

As far as the primary oscillatory flow in the Stokes layer is concerned, it is first of all of the interest to note that no net oscillatory viscous torque (at least to leading order) is exerted upon the sphere in spite of a three-dimensional character of the oscillation: $\boldsymbol{\Gamma}^{(u)} = \boldsymbol{0}$ (cf. §§2.2 and 2.3 for conventions). This follows from the linearity of the problem for the primary oscillatory flow and the fact of having just a superposition of two uniaxial vibrations, each one of which yields no torque. Thus, $\boldsymbol{\Omega}^{(u)} = \boldsymbol{0}$ (no torsional oscillations), should the sphere be even much lighter than the surrounding fluid and free to rotate. Along with a sphere free to rotate, we shall also consider the case of a 'fixed' sphere, for which $\boldsymbol{\Omega} \equiv \boldsymbol{0}$, no matter what the value of $\boldsymbol{\Gamma}$ is. As $\boldsymbol{\Gamma}^{(u)} = \boldsymbol{0}$, there is no difference between these two cases for the primary oscillatory flow. Yet the difference does appear for steady contributions, as seen below.

With torsional vibrations ruled out, the general results of §2 are applicable here. Thus, we can spare ourselves the effort of considering the Stokes layer (first for the

primary oscillatory flow and then for the inner steady streaming) as the inner-streaming characteristics of interest, the effective slip velocity and the induced tangential stress at the sphere surface, can be inferred from (2.72) and (2.73) by substituting (3.35) therein. After some simple algebra, the results can be written as

$$\Delta \boldsymbol{v}_{ts}^{(s)} = \tfrac{45}{32}\nabla_{ts}\left|\boldsymbol{u}_{\infty}^{(u1)}\cdot\boldsymbol{e}_r\right|^2 + \tfrac{27}{16}\mathrm{i}\left[\overline{\boldsymbol{u}_{\infty}^{(u1)}}\times\boldsymbol{u}_{\infty}^{(u1)}\right]\times\boldsymbol{e}_r, \tag{3.36}$$

$$\Delta \boldsymbol{\sigma}_{ts}^{(s)} = -\tfrac{9}{32}\sqrt{2}\nabla_{ts}\left|\boldsymbol{u}_{\infty}^{(u1)}\cdot\boldsymbol{e}_r\right|^2 + \tfrac{9}{16}\sqrt{2}\mathrm{i}\left[\overline{\boldsymbol{u}_{\infty}^{(u1)}}\times\boldsymbol{u}_{\infty}^{(u1)}\right]\times\boldsymbol{e}_r, \tag{3.37}$$

where

$$\nabla_{ts}\left|\boldsymbol{u}_{\infty}^{(u1)}\cdot\boldsymbol{e}_r\right|^2 = \boldsymbol{u}_{\infty}^{(u1)}\left(\overline{\boldsymbol{u}_{\infty}^{(u1)}}\cdot\boldsymbol{e}_r\right) + \overline{\boldsymbol{u}_{\infty}^{(u1)}}\left(\boldsymbol{u}_{\infty}^{(u1)}\cdot\boldsymbol{e}_r\right) - 2\left|\boldsymbol{u}_{\infty}^{(u1)}\cdot\boldsymbol{e}_r\right|^2\boldsymbol{e}_r, \tag{3.38}$$

although we prefer to keep the surface-gradient form in (3.36) and (3.37).

We observe that both the quantities (3.36) and (3.37) consist of a surface-potential part (surface gradient of a scalar quantity) and a rotational (torsional) part. Interestingly enough, the latter is exactly in the form of a rigid-body rotation and it is the vector (3.31) that is involved therein without changing sign, so that the sense of the rotation coincides with that of the elliptic orbit in the primary oscillation. On account of $|\boldsymbol{u}_{\infty}^{(u1)}\cdot\boldsymbol{e}_r|^2 = (u_{\infty 1}^{(u1)})^2(\boldsymbol{e}_1\cdot\boldsymbol{e}_r)^2 + (u_{\infty 2}^{(u1)})^2(\boldsymbol{e}_2\cdot\boldsymbol{e}_r)^2$, the surface-potential part is just a linear combination of two axisymmetric contributions with the axes along $\boldsymbol{e}_1$ and $\boldsymbol{e}_2$, each one for the corresponding constitutive uniaxial oscillation. In light of this, the rotational part can be interpreted as the 'cross-term' between the primary uniaxial oscillations. The distributions (3.36) and (3.37) are axisymmetric as a whole not only in the genuinely uniaxial case, but also in the circular-polarization case, with the symmetry axis given by $\boldsymbol{e}_3$ in the latter, for $|\boldsymbol{u}_{\infty}^{(u1)}\cdot\boldsymbol{e}_r|^2 = (u_{\infty}^{(u1)})^2[1-(\boldsymbol{e}_3\cdot\boldsymbol{e}_r)^2]$, even though the vector field directions of (3.36) and (3.37) are opposite in the meridional plane between these two cases. Another noteworthy feature is that the second terms in (3.36) and (3.37) are of the same sign, whereas the first terms are of different signs. This is explained by the fact that the surface-potential part of the inner streaming contains a recirculation zone, much in the same way such a zone exists in the uniaxial case (Riley 1966). The effective slip velocity represents the inner streaming at the outer edge of the Stokes layer, while the tangential stress acts on the boundary itself. Thus, as a result of the recirculation, their signs are different. However, there is no such recirculation for the rotational part of the inner streaming, which was pointed out by Lee & Wang (1989) in different terms.

The rotational part of (3.37) gives rise to a net steady torque exerted upon the sphere: $\boldsymbol{\Gamma}^{(s)} = \oint \boldsymbol{e}_r\times\Delta\boldsymbol{\sigma}_{ts}^{(s)}\,\mathrm{d}A$, where the integration is carried out over the whole surface area $r=1$. Using here (3.37) and the identity $\oint \boldsymbol{e}_r\boldsymbol{e}_r\,\mathrm{d}A = \frac{4\pi}{3}\boldsymbol{I}$, one finally obtains

$$\boldsymbol{\Gamma}^{(s)} = \frac{3\pi}{\sqrt{2}}\mathrm{i}\left[\overline{\boldsymbol{u}_{\infty}^{(u1)}}\times\boldsymbol{u}_{\infty}^{(u1)}\right], \quad \langle\boldsymbol{\Gamma}^{*}\rangle = \frac{\rho^{*}U^{*2}l^{*3}}{M}\boldsymbol{\Gamma}^{(s)}, \tag{3.39}$$

where a dimensional expression is also provided invoking the conventions adopted in §§2.2 and 2.3 (and recall that l^{*} is the sphere radius here). As $\boldsymbol{\Gamma}^{s} \neq \boldsymbol{0}$ (with the exception of the uniaxial case), emerging at this stage is a difference between the cases of a fixed sphere and the one free to rotate (cf. earlier discussion).

Consider first a *fixed* sphere. In this case, a steady flow in the main bulk (the outer streaming) is due exclusively to the effective slip velocity (3.36). The boundary conditions for the tangential and normal velocity components of this flow at the sphere surface are given by (2.64) and (2.67), where $\boldsymbol{u}^{(s)} = \boldsymbol{0}$ (the sphere is at rest) and

$\Delta \boldsymbol{v}_{ts}^{(s)}$ is given by (3.36). The boundary condition at infinity is $\boldsymbol{v}^{(s)} \to \boldsymbol{0}$. The equations governing the outer streaming are actually not the ordinary steady Navier–Stokes equations, but rather a slightly modified version thereof (Dore 1976; Riley 1992, 2001). Nevertheless, in the present paper we shall limit ourselves to the solution in the Stokes approximation ($R_s \ll 1$), which is not subjected to such modifications. Here $R_s = (\varepsilon U^*) l^*/\nu^* = \varepsilon^2 M^2$ is the streaming Reynolds number (Riley 1966), which can in principle take whatever value while $\varepsilon \ll 1$ and $M \gg 1$. We proceed from the general solution of the Stokes equations in the spherical coordinates given by Lamb (1932), of which the form given by Happel & Brenner (1965) better suits the present vector-form representation. We finally obtain

$$\boldsymbol{v}_{fixed}^{(s)} = \frac{27}{16r^2}\mathrm{i}\left[\overline{\boldsymbol{u}_\infty^{(u1)}} \times \boldsymbol{u}_\infty^{(u1)}\right] \times \boldsymbol{e}_r + \frac{45}{32r^4}\nabla_{ts}\left|\boldsymbol{u}_\infty^{(u1)} \cdot \boldsymbol{e}_r\right|^2 + \frac{135}{32}\left(\frac{1}{r^2} - \frac{1}{r^4}\right)\left[\left|\boldsymbol{u}_\infty^{(u1)} \cdot \boldsymbol{e}_r\right|^2 - \frac{1}{3}\left|\boldsymbol{u}_\infty^{(u1)}\right|^2\right]\boldsymbol{e}_r, \quad (3.40)$$

where recall that the surface-gradient term can be developed with the help of (3.38). In view of the linearity of the Stokes equations, the structure of (3.40) is clearly the same as that of (3.36) and (3.37) discussed above: a rotation part and two axisymmetric contributions corresponding to the uniaxial oscillations along $\boldsymbol{e}_1$ and $\boldsymbol{e}_2$. The other comments concerning the structure made following (3.36) and (3.37) are also valid. In particular, the flow field (3.40) is axisymmetric in the circular-polarization case with the flow direction in the meridional plane being opposite to that in the uniaxial case. The decay far away from the sphere is $O(r^{-2})$ for this and for the other outer streaming flows presented in this subsection (cf. the discussion following (3.21)).

The results (3.39) and (3.40) (as well as equivalents of (3.36) and (3.37)) have earlier been obtained by Lee & Wang (1989). They proceeded in a componentwise form, which generally made the developments more cumbersome. To recover their form of the results, one must use the representation $\boldsymbol{u}_\infty^{(u1)} = [(u_{\infty 1}^{(u1)})'\boldsymbol{e}_1' + (u_{\infty 2}^{(u1)})'\mathrm{e}^{\mathrm{i}\psi}\boldsymbol{e}_2']\,\mathrm{e}^{\mathrm{i}\psi_0'}$ and then the appropriate coordinate projections. Here the primes are added just to distinguish from the representation provided in the beginning of the present subsection, for which $\psi \equiv -\pi/2$ (which can always be achieved by turning the orthonormal basis $\{\boldsymbol{e}_1', \boldsymbol{e}_2'\}$ by an appropriate angle around the $\boldsymbol{e}_3 = \boldsymbol{e}_1' \times \boldsymbol{e}_2'$ axis).

In contrast to a fixed sphere, a sphere *free to rotate* will rotate under the torque (3.39). In the Stokes approximation, the part of the steady velocity field due to the sphere rotation is $\boldsymbol{v}_{rot}^{(s)} = (1/r^2)\boldsymbol{\Omega}^{(s)} \times \boldsymbol{e}_r$, and using (3.39) one can obtain

$$\boldsymbol{\Omega}^{(s)} = \tfrac{3}{16}\sqrt{2}M\mathrm{i}\left[\overline{\boldsymbol{u}_\infty^{(u1)}} \times \boldsymbol{u}_\infty^{(u1)}\right]. \quad (3.41)$$

First of all, one notices here the appearance of an asymptotically large parameter $M \gg 1$. In other words, the rotation is $O(M)$ times more intense than the intrinsic inner streaming ($\boldsymbol{\Omega}^{(s)} \gg 1$). This has been earlier established by Rednikov *et al.* (2003), who have also pointed out that the appropriate Reynolds number is now rather $\tilde{R}_s = \varepsilon^2 M^3$ (instead of R_s). They have also analysed the solution for $\boldsymbol{\Omega}^{(s)}$ at $\tilde{R}_s \gg 1$, which remains asymptotically large: $\boldsymbol{\Omega}^{(s)} = O(\varepsilon^{-2/3}) \gg 1$.

There is a particular case, however, when $\boldsymbol{\Omega}^{(s)} = O(1)$. It is the 'quasi-uniaxial' case, when $|\overline{\boldsymbol{u}_\infty^{(u1)}} \times \boldsymbol{u}_\infty^{(u1)}| \ll 1$ (in other words, $u_{\infty 1}^{(u1)} = O(1)$ while $u_{\infty 2}^{(u1)} \ll 1$, or *vice versa*). The outer streaming is then engendered by two contributions of the same order of magnitude: from an axisymmetric (to leading order, on account of $u_{\infty 2}^{(u1)} \ll 1$) distribution of the effective slip velocity and a sphere rotation, the symmetry axis for the former being orthogonal to the rotation axis. Thus, the quasi-uniaxial case is

clearly a distinguished asymptotic limit for a sphere free to rotate (but not for a fixed sphere).

On the other hand, in spite of generally $|\boldsymbol{\Omega}^{(s)}| \gg 1$, the streaming contribution from the effective slip velocity may still be of interest as it accounts for a topologically different flow structure. This is first of all true for small streaming Reynolds numbers, for the leading-order flow $\boldsymbol{v}^{(s)}_{rot} = (1/r^2)\boldsymbol{\Omega}^{(s)} \times \boldsymbol{e}_r$ consists of closed streamlines. As such, it plays no role in, e.g. the streaming-induced convective mass/heat transfer from the sphere (spherically symmetric when purely conductive). Thus, with the attention limited to $\tilde{R}_s \ll 1$, the steady flow field for a sphere free to rotate is given by

$$\boldsymbol{v}^{(s)}_{free} = \boldsymbol{v}^{(s)}_{rot} + \boldsymbol{v}^{(s)}_{fixed}, \tag{3.42}$$

where $\boldsymbol{v}^{(s)}_{fixed}$ is defined in (3.40), the first term of which can be neglected for consistency versus $\boldsymbol{v}^{(s)}_{rot}$. In fact, as noted by Rednikov *et al.* (2003), for $\boldsymbol{v}^{(s)}_{rot}$, it is expedient to include not only the already mentioned leading-order part $\boldsymbol{v}^{(s)}_{rot} = (1/r^2)\boldsymbol{\Omega}^{(s)} \times \boldsymbol{e}_r$, but also a first correction in the small Reynolds number. Indeed, in view of $|\boldsymbol{\Omega}^{(s)}| \gg 1$, such a correction may well be $O(1)$ on the scale of $\boldsymbol{v}^{(s)}_{fixed}$. It is physically clear that it must be a kind of 'centrifugal' flow, directed from the rotation axis towards the equatorial plane while skirting the sphere surface. Thus, from the viewpoint of the flow topology discussed above, it contributes in a similar way to $\boldsymbol{v}^{(s)}_{fixed}$. The correction in question can easily be derived from the Navier–Stokes equations (cf. Rednikov *et al.* 2003) to yield

$$\boldsymbol{v}^{(s)}_{rot} = \frac{1}{r^2}\boldsymbol{\Omega}^{(s)} \times \boldsymbol{e}_r + \frac{1}{8}R_s\left(\frac{1}{r^4} - \frac{1}{r^3}\right)\nabla_{ts}\left(\boldsymbol{\Omega}^{(s)} \cdot \boldsymbol{e}_r\right)^2 + \frac{3}{8}R_s\left(\frac{2}{r^3} - \frac{1}{r^4} - \frac{1}{r^2}\right)\left[\left(\boldsymbol{\Omega}^{(s)} \cdot \boldsymbol{e}_r\right)^2 - \frac{1}{3}\left|\boldsymbol{\Omega}^{(s)}\right|^2\right]\boldsymbol{e}_r. \tag{3.43}$$

Thus, for the steady flow around a sphere free to rotate, we finally have (3.42) with (3.40), (3.41) and (3.43). We note that the difference with the case of a fixed sphere eventually reduces just to the value (or more correctly, the order of magnitude) of the angular velocity involved, although this is an essential difference. For a fixed sphere, the apparent angular velocity in the outer streaming (even though the sphere itself is motionless) is imposed by the effective slip velocity (3.36) and is much smaller than (3.41) for a sphere free to rotate, for which it is imposed by the induced tangential stress (3.37) resulting in a net torque (3.39).

The result (3.42) can be generalized in a rather straightforward manner to the case of a *liquid* sphere (spherical drop) whose density and dynamic viscosity are much greater than those of the outside fluid (e.g. a drop in air). The latter requirements are essential, for in this case the primary oscillatory flow does not 'penetrate' into the drop to leading order, thus remaining the same as for a rigid sphere. Consequently, the inner-streaming results such as (3.36) and (3.37) are still applicable. However, as far as the steady flow is concerned, the 'liquidity' of the sphere may become apparent even if the outside-to-inside viscosity ratio, δ_η, is small ($\delta_\eta \ll 1$), as required here. Indeed, the part of the induced tangential stress (3.37) that is not offset by the rigid-body rotation must be assumed by an internal circulation in the drop. As we shall see shortly, its intensity may well be of the same order of magnitude as the effective slip velocity ($O(1)$ in the scalings used here), which would modify the corresponding part of (3.42). On the other hand, the internal circulation is of importance by itself, irrespective of whether or not it brings about tangible consequences for the outside flow.

Let the hat notation distinguish the velocity field inside the drop from the one outside, the scalings being the same, $[\hat{\boldsymbol{v}}] = [\boldsymbol{v}]$. In the limit of small streaming Reynolds numbers, the rotational part of the induced tangential stress (3.37) gets balanced by the viscous stresses from the outside of the drop due to its rigid-body rotation (this part cannot be balanced by viscous stresses from the inside of a *spherical* drop, even though $\delta_\eta \ll 1$), while the surface-potential part gets balanced by viscous stresses due to the internal circulation (here the outside contribution is neglected in view of $\delta_\eta \ll 1$). Thus,

$$-\frac{9}{32}\sqrt{2}\nabla_{\tau s}\left|\boldsymbol{u}_\infty^{(u1)}\cdot\boldsymbol{e}_r\right|^2 = \frac{1}{M_\eta}\left(\frac{\partial\hat{\boldsymbol{v}}_\tau^{(s)}}{\partial r} - \hat{\boldsymbol{v}}_\tau^{(s)}\right) \qquad \text{at} \quad r=1, \tag{3.44}$$

where the notation $M_\eta = M\delta_\eta$ has been introduced following Rednikov *et al.* (2003). While $M \gg 1$ and $\delta_\eta \ll 1$, the parameter M_η can in principle take any value, large or small. The solution of the Stokes equations inside the drop satisfying (3.44) and $\hat{v}_n^{(s)} = 0$ at $r = 1$ is

$$\hat{\boldsymbol{v}}^{(s)} = \boldsymbol{\Omega}^{(s)}\times\boldsymbol{e}_r r + \frac{9}{320}\sqrt{2}M_\eta\left(3r-5r^3\right)\nabla_{\tau s}\left|\boldsymbol{u}_\infty^{(u1)}\cdot\boldsymbol{e}_r\right|^2 + \frac{27}{160}\sqrt{2}M_\eta(r-r^3)\left[\left|\boldsymbol{u}_\infty^{(u1)}\cdot\boldsymbol{e}_r\right|^2 - \frac{1}{3}\left|\boldsymbol{u}_\infty^{(u1)}\right|^2\right]\boldsymbol{e}_r. \tag{3.45}$$

The above two boundary conditions are satisfied for any $\boldsymbol{\Omega}^{(s)}$, but its value is given by (3.41) as considered earlier. The first term on the right-hand side of (3.45) represents a rigid-body rotation of the drop, whereas the rest of the terms account for the internal circulation. The former is much ($\delta_\eta^{-1} \gg 1$ times) more intense than the latter in the general case, even though the two may become of the same order in the quasi-uniaxial case. In the uniaxial case, $\boldsymbol{\Omega}^{(s)} = \boldsymbol{0}$, the internal circulation is axisymmetric, and the result of Zhao *et al.* (1999*a*) is recovered. In the circular-polarization case, on the other hand, when the corresponding result of Rednikov, Riley & Sadhal (2003) is recovered, the flow (3.45) is once again axisymmetric, albeit with $\boldsymbol{\Omega}^{(s)} \neq \boldsymbol{0}$ and the sense of the internal circulation just opposite to the uniaxial case. The latter is not surprising given that we have already pointed out such a correlation between these two limiting cases on a few occasions.

Let us note, however, that the boundary condition (3.44) is valid in this form only at $\tilde{R}_s \ll 1$. At finite $\tilde{R}_s$, its left-hand side should actually be replaced by $(\boldsymbol{\sigma}_{\tau s}^{(s)}|_{RBR} + \Delta\boldsymbol{\sigma}_{\tau s}^{(s)})$, where the first term refers to the distribution of the viscous tangential stress exerted on the surface of the sphere due to its steady rigid-body rotation. At $\tilde{R}_s = 0$, $\boldsymbol{\sigma}_{\tau s}^{(s)}|_{RBR}$ exactly offsets the rotational part of (3.37), and we arrive at (3.44).

We are now in a position to consider how the liquidity of the sphere (*viz.* the internal circulation) modifies the steady flow outside of it. This comes through the tangential-velocity condition (2.64), where $\boldsymbol{u}_\tau^{(s)}$ is now affected by the internal circulation: $\boldsymbol{u}_\tau^{(s)} = \hat{\boldsymbol{v}}_{\tau s}^{(s)}$. On account of (3.45), the small-Reynolds-number steady flow outside a liquid sphere is shown as

$$\boldsymbol{v}_{liq}^{(s)} = \boldsymbol{v}_{rot}^{(s)} + \frac{45}{32}\left(1-\frac{1}{25}\sqrt{2}M_\eta\right)\frac{1}{r^4}\nabla_{\tau s}\left|\boldsymbol{u}_\infty^{(u1)}\cdot\boldsymbol{e}_r\right|^2 + \frac{135}{32}\left(1-\frac{1}{25}\sqrt{2}M_\eta\right)\left(\frac{1}{r^2}-\frac{1}{r^4}\right)\left[\left|\boldsymbol{u}_\infty^{(u1)}\cdot\boldsymbol{e}_r\right|^2 - \frac{1}{3}\left|\boldsymbol{u}_\infty^{(u1)}\right|^2\right]\boldsymbol{e}_r, \tag{3.46}$$

where $\boldsymbol{v}_{rot}^{(s)}$ is still given by (3.43). We observe that M_η is the key parameter as far as the effect of the sphere's liquidity is concerned: for $M_\eta = 0$ the result (3.42) is recovered, whereas for sufficiently large M_η ($M_\eta > 25/\sqrt{2}$) the internal circulation exceeds the effective slip velocity in intensity so that the sense of the corresponding part of the flow gets reversed. This 'critical' value of M_η is independent of the oscillation type and was earlier established in the uniaxial (Zhao *et al.* 1999*a*) and circular-polarization (Rednikov *et al.* 2003) cases. Note that the internal circulation being directed in the opposite sense to the effective slip velocity is a consequence of the opposite signs of the surface-potential parts of (3.36) and (3.37).

To wrap up this subsection, we carry out a small parametric study of the axisymmetric small-Reynolds-number steady-flow patterns occurring in the framework of the present analysis. Since they are axisymmetric just in the uniaxial and circular-polarization cases, a first parameter is defined to discriminate between these two cases in the expressions that follow: $n \equiv 0$ (uniaxial) and $n \equiv 1$ (circular polarization). Another parameter is obviously M_η. At last, we have $\delta_R \equiv R_s M^2 = \varepsilon^2 M^4$ characterizing the relative importance, within (3.46), of $\boldsymbol{v}_{rot}^{(s)}$ in the *meridional* plane (a plane passing through the symmetry axis). Note that it is actually the correction terms (here referred to as the centrifugal flow) in (3.43) that possess meridional-plane components, the leading-order term accounting for a purely azimuthal flow (orthogonal to this plane). It is in the meridional plane that the streamlines are shown below, it being understood that in the circular-polarization case there is also an azimuthal component of the flow. It is convenient to represent the results in terms of the stream function (3.16), the spherical coordinates being based upon the symmetry axis. At this stage, it is also convenient to concretize the velocity scale U^* earlier left unspecified: we choose $U^* = u_\infty^{(u1)*}$ such that $u_\infty^{(u1)} \equiv 1$. As it can be deduced from (3.45) and (3.46) with (3.41) and (3.43), the steady meridional-plane flow outside and inside the sphere is given by

$$\psi^{(s)} = [1-(-1)^n]\,\frac{9}{512}\delta_R\left(\frac{2}{r}-\frac{1}{r^2}-1\right)\cos\theta\sin^2\theta + (-1)^n\left(\frac{45}{32}-\frac{9}{160}\sqrt{2}M_\eta\right)\left(1-\frac{1}{r^2}\right)\cos\theta\sin^2\theta, \quad (3.47)$$

$$\hat{\psi}^{(s)} = (-1)^n\frac{9}{160}\sqrt{2}M_\eta(r^3-r^5)\cos\theta\sin^2\theta. \quad (3.48)$$

The streamlines are shown (at the interval 0.016) in figure 2 for certain representative values of the parameters. Each time, just one quadrant is displayed on account of an additional symmetry, with respect to the equatorial plane (horizontal on the diagrams). Note the opposite directions of the flow between the uniaxial and circular-polarization cases. As the internal circulation is increased, the flow outside the sphere first drops in intensity and then reverses its direction. The centrifugal flow (characterized by δ_R) is directed in the same way as the effective slip velocity, and thus the overall flow intensity grows with δ_R. Should the internal circulation be as intense as to reverse the flow outside the sphere, the centrifugal contribution nonetheless dominates at larger distances. This results in a recirculation zone observed in figure 2(*i*). Let us finally note that the case of a fixed sphere, (3.40), formally corresponds to $\delta_R \equiv 0$ in this framework, irrespective of the actual value taken by δ_R (cf. the discussion on the angular velocity following (3.43)). Besides, a fixed sphere is considered just as being rigid ($M_\eta = 0$). Thus, the fixed-sphere case is exhausted by the first two diagrams in the first row of figure 2.

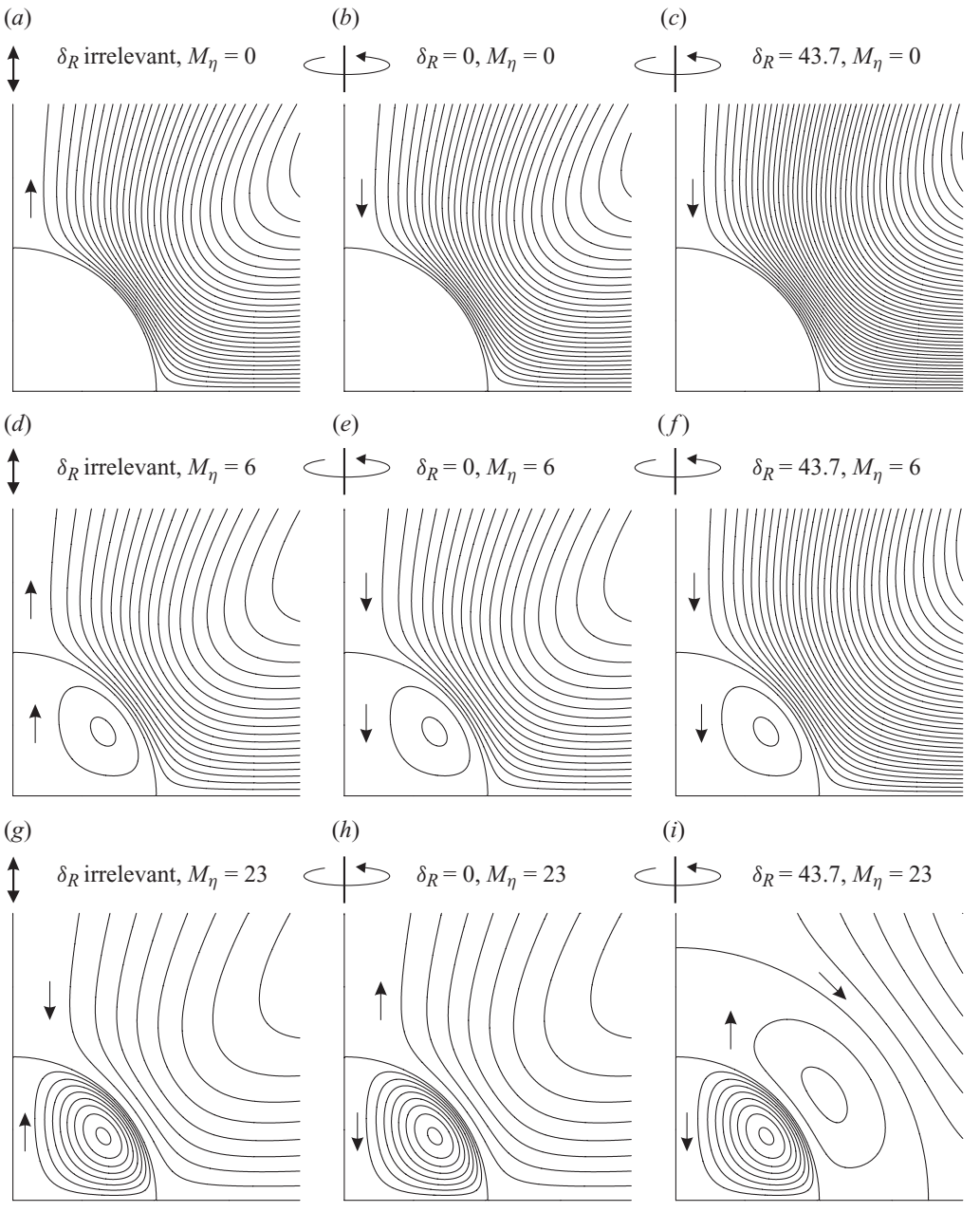

FIGURE 2. Axisymmetric low-Reynolds-number steady streaming patterns, (3.47) and (3.48), arising on the background of a high-frequency translational oscillation between a rigid sphere/viscous spherical drop and an incompressible fluid medium ((*a*, *d*, *g*) for the uniaxial case, (*b*, *e*, *h* and *c*, *f*, *i*) for the circular-polarization one). M_η characterizes the 'liquidity' of the sphere, while δ_R the 'centrifugal' effect of the rigid-body rotation. Arrows indicate the flow direction.

3.5. *Torque on a circular disk in two orthogonal standing waves*

Here we revisit the problem treated by Busse & Wang (1981). Consider two orthogonal plane acoustic standing waves (of the same frequency) in the x and y directions,

respectively. The complex amplitude of the potential can be written as

$$\varphi^{(u1)} = \frac{1}{k} U_x \sin kx + \frac{1}{k} U_y \, \mathrm{e}^{-\mathrm{i}\psi} \sin ky, \tag{3.49}$$

where U_x and U_y are the wave amplitudes, and ψ is the phase angle between the waves. A thin circular disk is placed into the acoustic field, with its axis being in the z-direction, such that $\{x, y, z\}$ is a (right-handed) Cartesian system of coordinates. The length scale l^* is the radius of the disk. The velocity scale U^* is a quantity of the order of the velocity amplitude of the waves. The coordinates of the centre of the disk are $x = x_0$, $y = y_0$, which can be arbitrary. The goal of the present subsection is to calculate the steady torque on the disk (with respect to the disk axis), which in the present configuration is entirely due to the tangential stress rather than the steady (radiation) pressure (Busse & Wang 1981). Similar to Busse & Wang (1981), the disk is treated as infinitesimally thin, and possible edge effects are neglected.

To calculate the distribution of the tangential stress on the plane of the disk, the general result (2.70) is used, where

$$\boldsymbol{v}_{\tau s}^{(u1)} = U_x \cos kx \boldsymbol{e}_x + U_y \, \mathrm{e}^{-\mathrm{i}\psi} \cos ky \boldsymbol{e}_y, \tag{3.50}$$

$$p_s^{(u1)} = -\frac{\mathrm{i}}{k} U_x \sin kx - \frac{\mathrm{i}}{k} U_y \, \mathrm{e}^{-\mathrm{i}\psi} \sin ky, \tag{3.51}$$

$$\nabla_{\tau s} = \boldsymbol{e}_x \frac{\partial}{\partial x} + \boldsymbol{e}_y \frac{\partial}{\partial y} \tag{3.52}$$

are substituted with $\boldsymbol{e}_x$ and $\boldsymbol{e}_y$ being the unit vectors in the x and y directions, respectively. We obtain

$$\begin{aligned} \Delta\boldsymbol{\sigma}_{\tau s}^{(s)} = {} & \frac{1}{2\sqrt{2}} k U_x U_y \sin\psi \left(1 + \frac{R_T}{Pr^{1/2}}\right) (-\cos kx \sin ky \boldsymbol{e}_x + \sin kx \cos ky \boldsymbol{e}_y) \\ & + \frac{1}{2\sqrt{2}} k U_x U_y \cos\psi \frac{R_T}{Pr^{1/2}} (\cos kx \sin ky \boldsymbol{e}_x + \sin kx \cos ky \boldsymbol{e}_y) + O\left(U_x^2; U_y^2\right), \end{aligned} \tag{3.53}$$

where only the 'cross-term', with $U_x U_y$, is retained, for it is clear from symmetry considerations that the terms with U_x^2 and U_y^2 do not contribute into the torque.

If $\{z, \varrho, \phi\}$ is the cylindrical coordinate system such that

$$x = x_0 + \varrho \cos\phi, \quad y = y_0 + \varrho \sin\phi, \tag{3.54}$$

the torque on the disk (whose only non-zero component is in the z-direction) is calculated as

$$\Gamma_z^{(s)} = 2 \int_{-\pi}^{\pi} \mathrm{d}\phi \int_0^1 \mathrm{d}\varrho \varrho^2 \boldsymbol{e}_z \cdot \left(\boldsymbol{e}_\varrho \times \Delta\boldsymbol{\sigma}_{\tau s}^{(s)}\right). \tag{3.55}$$

Here the factor '2' accounts for the two sides of the disk; $\boldsymbol{e}_z$ and $\boldsymbol{e}_\varrho$ are the unit vectors along z and ϱ, respectively. Next, (3.53) should be substituted into (3.55) taking into account (3.54) and

$$\boldsymbol{e}_z \cdot (\boldsymbol{e}_\varrho \times \boldsymbol{e}_x) = -\sin\phi, \quad \boldsymbol{e}_z \cdot (\boldsymbol{e}_\varrho \times \boldsymbol{e}_y) = \cos\phi. \tag{3.56}$$

The integral with respect to ϕ can be significantly simplified on account of symmetries.

The result is

$$\Gamma_z^{(s)} = \sqrt{2}\left(1 + \frac{R_T}{Pr^{1/2}}\right) kU_x U_y \sin\psi \cos kx_0 \cos ky_0 \times \int_{-\pi}^{\pi} \mathrm{d}\phi \cos\phi \int_0^1 \mathrm{d}\varrho \varrho^2 \sin(k\varrho\cos\phi)\cos(k\varrho\sin\phi). \quad (3.57)$$

If the disk is small as compared to the acoustic wavelength, $k \ll 1$, then (3.57) can be developed as

$$\Gamma_z^{(s)} = \frac{\sqrt{2}\pi}{4}\left(1 + \frac{R_T}{Pr^{1/2}}\right) U_x U_y \sin\psi \cos kx_0 \cos ky_0 k^2 \left(1 - \frac{k^2}{6} + O(k^4)\right). \quad (3.58)$$

Interestingly enough, the expansion starts with the term $O(k^2)$, with no $O(k^0)$ term present. Thus, for a thin disk and with the edge effects neglected, there is no torque generated in the incompressible limit. This is what should have been expected. Indeed, if (2.33) is considered in the incompressible case with a constant vector $\boldsymbol{v}_{ts}^{(u1)}$ near a plane surface, it corresponds to an exact solution (purely oscillatory) of the Navier–Stokes equations, and thus no steady component is generated at all.

In the dimensional form, the torque is (cf. §§ 2.2 and 2.3)

$$\langle \Gamma_z^* \rangle = \frac{\rho^* U^{*2} l^{*3}}{M} \Gamma_z^{(s)}. \quad (3.59)$$

Without the non-adiabatic contribution ($R_T = 0$), the result (3.58) coincides with Busse & Wang (1981). Making estimations similar to § 3.1, we establish that, e.g. for diatomic ideal gases with $Pr = 1$, the non-adiabatic effect of compressibility brings about a +40 % effect on the torque value. Unfortunately, such an increase seems to push the theoretical result even further from the corresponding experimental result shown by Busse & Wang (1981, figure 1).

4. Concluding remarks

In the present paper, we have considered a generalized approach to the inner streaming near a motionless boundary, as well as examples of its application to a number of particular problems of interest. In each of these examples, any detailed calculation of the inner streaming could be avoided, owing to the availability of the generalized results. Within each particular problem, the analysis has been carried out in the following way. First, the (irrotational) primary oscillatory flow in the main bulk of the fluid (i.e. outside the infinitesimally thin Stokes layer at the boundary) is considered. Its amplitude evaluated at the boundary is then used in the generalized results to infer the relevant inner-streaming characteristics. After that, the outer streaming and maybe some other steady effects could be studied.

The relevant inner-streaming characteristics are the effective slip velocity and the induced tangential stress acting on the boundary. Within the generalized treatment, and for an arbitrary smooth boundary, the distributions of both characteristics along the boundary have been expressed through a similar distribution of the amplitude of the main-bulk primary oscillatory flow evaluated at the boundary. The vector form of the analysis has proved effective here. The final results are more compact and easy to grasp than similar results in Lee & Wang (1989), which were developed in a component form. Apparently, another reason for that is a certain additional simplification achieved here by making use of the irrotationality of the

primary oscillatory velocity field (*viz*. the identity proven in the Appendix). Note that the results of Lee & Wang (1989) also contain terms associated with the normal velocity of the boundary, the effect of which has not been included in the present study.

Five contributions can be distinguished according to their physical interpretation within the result for the effective slip velocity obtained here. First, it is the 'incompressible' contribution (part I). It is only this term that remains either in the truly incompressible case (and with the coefficient of viscosity being constant), or rather when the Stokes layer is formally treated as incompressible (e.g. done in the book by Landau & Lifshitz (1988) for a genuinely compressible situation). Other terms owe themselves either to compressibility, or to variability of the coefficient of viscosity (which is a function of the temperature and pressure oscillating in the acoustic wave). Furthermore, there are adiabatic and non-adiabatic contributions to these effects. Thus, we have terms associated with the adiabatic effect of compressibility (part IIa) and of variable viscosity (part IIb), as well as the non-adiabatic effect of compressibility (part IIIa) and of variable viscosity (part IIIb). The authors are not aware of any other studies in the literature where the effects associated with all the five parts would be taken into consideration. Speaking in these terms, the results by Nyborg (1958), Lee & Wang (1989); Lee & Wang (1990), Zhao *et al*. (1999*b*) contain just parts I and IIa. Gopinath & Trinh's (2000) results include I, IIa and IIIa. Parts I, IIa and IIb can be traced within the analysis of Yarin *et al*. (1999).

It turns out though that only parts I and IIIa are present in the result for the induced tangential stress, with the contributions due to the other parts identically vanishing.

In the case when the primary oscillatory flow is all in phase to leading order (as in an acoustic standing wave), parts IIa and IIb vanish within the result for the effective slip velocity. Thus, apart from the incompressible term (part I), only the non-adiabatic contributions remain (parts IIIa and IIIb). For gases, it turns out that parts IIIa and IIIb tend to offset each other, thus reducing the overall non-adiabatic contribution. For ideal gases, and with the coefficient of viscosity being proportional to the square root of the absolute temperature, the sum of IIIa and IIIb turns out to be just one half of IIIa. For liquids, part IIIa is practically negligible (just to the extent the relative difference between heat capacities at constant pressure and at constant volume is small). Nonetheless, part IIIb (associated with the non-adiabatic viscosity variability) may be significant. The point is that, for liquids, the coefficient of viscosity is typically much more sensitive to temperature than the density is. Accordingly, part IIIb is expected to be much greater than part IIIa, the latter being regarded negligible. The above concerned the effective slip velocity. For the induced tangential stress, where only parts I and IIIa are present in any case (irrespective of whether the wave is standing), the non-adiabatic contribution is negligible for liquids, in view of what has just been said in regard to part IIIa for liquids. But for gases, this could now give rise to a significant non-adiabatic contribution, which is partly because part IIIb is not there to offset part IIIa.

As an example, the classical problem of a plane standing wave grazing a wall parallel to its direction has been considered. The importance of the non-adiabatic contribution has been estimated for this particular problem. For this purpose, the sum of parts IIIa and IIIb is evaluated as a fraction of part I within the expression for the effective slip velocity, and the sign is retained to indicate whether the overall non-adiabatic effect amplifies (+) or reduces (−) the streaming characteristic in question. The result is approximately +11 % for monoatomic ideal gases, and +7 %

for diatomic ideal gases (with the Prandtl number equal to unity). This is not very significant, but still noticeable. For water at 20 °C, the estimation yields approximately +18 %, which becomes +25 % for water at 30 °C. This is rather appreciable, which is quite a surprising result. This shows that, for liquids, the non-adiabatic effect of variable viscosity is always worth estimating. A great diversity of the result is expected for liquids. This is unlike gases, for which it lies more or less within the same bounds irrespective of a particular gas considered. Note, however, that the above estimations are strictly for the case when the wall is much more heat-conducting than the fluid. While seemingly a solid assumption for gases, it may not always be so for liquids. If it is not so, then the non-adiabatic contribution is lower than the above estimations. For the induced tangential stress, similar estimations yield −67 % for monoatomic ideal gases, and −40 % for diatomic ideal gases (with the Prandtl number equal to unity). This is already significant, much more so than for the effective slip velocity in the case of gases. For liquids, on the other hand, the non-adiabatic effect is negligible within the induced tangential stress, as it has been discussed earlier.

As another example, steady streaming from a small sphere placed at a certain position in a plane acoustic standing wave has been considered. A most notable new result here is a leading-order expression for the steady streaming uniformly valid for an arbitrary position of the sphere within the standing wave, from the velocity antinode to the velocity node.

A similar problem for the oblate spheroid (with the axis aligned with the wave) has also been treated, albeit just in the incompressible limit. This example has in particular illustrated the accessibility of the general formulas to coordinate systems more complex than just the Cartesian or spherical ones.

The example with three-dimensional translational oscillations of the sphere has illustrated the possibility and efficiency of adhering to a vector representation in an inherently three-dimensional situation up to later stages of the analysis. Beyond the form of the representation, new results here pertain to the outer streaming for the cases of a sphere free to rotate and a spherical drop more viscous than the medium (including the internal circulation and its influence on the steady flow outside the drop), which have not been considered for such a general form of oscillation before.

As a final example, the steady torque acting on a thin circular disk in two out-of-phase orthogonal plane acoustic standing waves, with the disk axis being orthogonal to the direction of the waves, has been calculated including a contribution due to the non-adiabatic effect of compressibility. For diatomic ideal gases with the Prandtl number equal to unity, its effect on the torque value is estimated at +40 %. However, such an increase in the theoretical value only seems to worsen the agreement with experiment, to judge by the experimental results plotted by Busse & Wang (1981).

All in all, the examples have demonstrated a significant simplification and systematization in the acoustic/steady streaming treatment achieved with the help of the generalized approach developed here. In the present paper, attention has been limited to the case of a motionless boundary, motionless just in the sense of primary oscillations, even though its motion has been allowed as far as the steady flow component is concerned. One direction for future work is to lift such a limitation, which would permit the coverage of a wider class of acoustic/steady streaming problems, including torsional oscillations and liquid–liquid interfaces.

The authors are grateful to NASA for financial support.

Appendix. Proof of the property (2.36)

The tangential vector $\boldsymbol{a}_\tau$ in (2.36) must be surface-potential

$$\boldsymbol{a}_\tau = \nabla_\tau \varphi, \tag{A 1}$$

whereas the corresponding three-dimensional vector field $\boldsymbol{a}$ (if any is associated with $\boldsymbol{a}_\tau$) need not be potential. In our way to (2.36), we consider a couple of commutation properties for the ∇_τ operator. With (2.17) and (2.19), one has $\nabla \boldsymbol{n} = \nabla_\tau \boldsymbol{n}$, which is a symmetric surface tensor, with only tangential components. This is used in the following manipulations.

First, a commutation rule for the operators ∇_τ and $\partial/\partial y$ is derived. With (2.17) and (2.19), we have

$$\frac{\partial}{\partial y}\nabla_\tau = \boldsymbol{n}\cdot\nabla(\nabla - \boldsymbol{n}\boldsymbol{n}\cdot\nabla), \tag{A 2}$$

where

$$\boldsymbol{n}\cdot\nabla\nabla = \nabla(\boldsymbol{n}\cdot\nabla) - (\nabla_\tau \boldsymbol{n})\cdot\nabla_\tau, \tag{A 3}$$

$$\boldsymbol{n}\cdot\nabla(\boldsymbol{n}\boldsymbol{n}\cdot\nabla) = \boldsymbol{n}\boldsymbol{n}\cdot\nabla(\boldsymbol{n}\cdot\nabla), \tag{A 4}$$

and thus

$$\frac{\partial}{\partial y}\nabla_\tau = \nabla_\tau \frac{\partial}{\partial y} - (\nabla_\tau \boldsymbol{n})\cdot\nabla_\tau, \tag{A 5}$$

which is the sought commutation rule.

Second, we are interested in the commutation of ∇_τ with itself. Let the subscripts $i, j = 1, 2, 3$ denote the Cartesian components of vector/tensor entities. The tensor operator $\nabla\nabla$ is symmetric

$$\nabla_i \nabla_j = \nabla_j \nabla_i, \tag{A 6}$$

since the operator ∇ is self-commutative. This not so for $\nabla_\tau\nabla_\tau$ as the operator ∇_τ is generally not commutative with itself. The substitution of (2.17) into (A 6) brings to

$$\nabla_{\tau i}\nabla_{\tau j} + n_i \frac{\partial}{\partial y} n_j \frac{\partial}{\partial y} + n_i \frac{\partial}{\partial y}\nabla_{\tau j} + \nabla_{\tau i}\left(n_j \frac{\partial}{\partial y}\right) = \nabla_{\tau j}\nabla_{\tau i} + n_j \frac{\partial}{\partial y} n_i \frac{\partial}{\partial y} + n_j \frac{\partial}{\partial y}\nabla_{\tau i} + \nabla_{\tau j}\left(n_i \frac{\partial}{\partial y}\right). \tag{A 7}$$

With (2.19), the second terms on each side of the equality are equal to each other and cancel out. Developing the last terms and taking into account that the tensor $\nabla_\tau \boldsymbol{n}$ is symmetric, i.e. $\nabla_{\tau i} n_j = \nabla_{\tau j} n_i$, an additional couple of terms cancels out, and the equality becomes

$$\nabla_{\tau i}\nabla_{\tau j} + n_i \frac{\partial}{\partial y}\nabla_{\tau j} + n_j \nabla_{\tau i}\frac{\partial}{\partial y} = \nabla_{\tau j}\nabla_{\tau i} + n_j \frac{\partial}{\partial y}\nabla_{\tau i} + n_i \nabla_{\tau j}\frac{\partial}{\partial y}. \tag{A 8}$$

Using (A 5) here, one finally obtains

$$\nabla_{\tau i}\nabla_{\tau j} - n_i(\nabla_{\tau j}\boldsymbol{n})\cdot\nabla_\tau = \nabla_{\tau j}\nabla_{\tau i} - n_j(\nabla_{\tau i}\boldsymbol{n})\cdot\nabla_\tau, \tag{A 9}$$

which is the sought commutation relation. To put it in different terms, it has been found that the tensor

$$\nabla_\tau\nabla_\tau - \boldsymbol{n}(\nabla_\tau \boldsymbol{n})\cdot\nabla_\tau \tag{A 10}$$

is symmetric (whereas $\nabla_\tau\nabla_\tau$ is generally not).

Now coming back to (2.36), and using (A 1) in that, one obtains

$$\boldsymbol{a}_\tau \cdot \nabla_\tau \boldsymbol{a}_\tau = (\nabla_\tau \varphi) \cdot \nabla_\tau \nabla_\tau \varphi = (\nabla_\tau \varphi) \cdot (\nabla_\tau \nabla_\tau \varphi - \boldsymbol{n}(\nabla_\tau \boldsymbol{n}) \cdot \nabla_\tau \varphi), \tag{A 11}$$

where an identically zero term (in view of $(\nabla_\tau \varphi) \cdot \boldsymbol{n} = 0$) has formally been added in. As the tensor (A 10) is symmetric, the left scalar product can be replaced by the right one, the above equality being continued in the following:

$$= (\nabla_\tau \nabla_\tau \varphi) \cdot \nabla_\tau \varphi - \boldsymbol{n}\, (\nabla_\tau \varphi) \cdot (\nabla_\tau \boldsymbol{n}) \cdot \nabla_\tau \varphi = \tfrac{1}{2} \nabla_\tau (\boldsymbol{a}_\tau \cdot \boldsymbol{a}_\tau) - \boldsymbol{n} \boldsymbol{a}_\tau \cdot (\nabla_\tau \boldsymbol{n}) \cdot \boldsymbol{a}_\tau. \tag{A 12}$$

Taking the tangential component here, the equality (2.36) is finally recovered.

REFERENCES

Amin, N. & Riley, N. 1990 Streaming from a sphere due to a pulsating source. *J. Fluid Mech.* **210**, 459–473.

Busse, F. H. & Wang, T. G. 1981 Torque generated by orthogonal acoustic waves – theory. *J. Acoust. Soc. Am.* **69**, 1634–1638.

Dore, B. D. 1976 Double boundary layers in standing surface waves. *Pure Appl. Geophys.* **114**, 629–637.

Gopinath, A. & Trinh, E. H. 2000 Compressibility effects on steady streaming from a non-compact rigid sphere. *J. Acoust. Soc. Am.* **108**, 1514–1520.

Happel, J. & Brenner, H. 1965 *Low Reynolds Number Hydrodynamics*. Prentice-Hall.

Kotas, C. W., Yoda, M. & Rogers, P. H. 2007 Visualization of steady streaming near oscillating spheroids. *Exp. Fluids* **42**, 111–121.

Lamb, H. 1932 *Hydrodynamics*. Cambridge University Press.

Landau, L. D. & Lifshitz, E. M. 1988 *Hydrodynamics* (in Russian). Nauka.

Lee, C. P., Anikumar, A. V. & Wang, T. G. 1994 Static shape of an acoustically levitated drop with wave–drop interaction. *Phys. Fluids* **6**, 3554–3566.

Lee, C. P. & Wang, T. G. 1989 Near-boundary streaming around a small sphere due to two orthogonal standing waves. *J. Acoust. Soc. Am.* **85**, 1081–1088.

Lee, C. P. & Wang, T. G. 1990 Outer acoustic streaming. *J. Acoust. Soc. Am.* **88**, 2367–2375.

Lee, Sungho, Sadhal, S. S. & Rednikov, A. Y. 2008 An analytical model of external streaming and heat transfer for a levitated flattened liquid drop. *J. Heat Transfer* **130**, 091602(1–8).

Lide, D. R. (ed.) 2003 *CRC Handbook of Chemistry and Physics*. CRC Press.

Lighthill, J. 1997 Introduction. In *Encyclopedia of Acoustics* (ed. M. J. Crocker), pp. 285–299. Wiley.

Lighthill, M. J. 1978 Acoustic streaming. *J. Sound Vib.* **61**, 391–418.

Marston, P. L. 1980 Shape oscillations and static deformation of drops and bubbles driven by modulated radiation stresses: theory. *J. Acoust. Soc. Am.* **67**, 15–26.

Nyborg, W. L. 1958 Acoustic streaming near a boundary. *J. Acoust. Soc. Am.* **30**, 329–339.

Nyborg, W. L. 1965 Acoustic streaming. In *Physical Acoustics. Principles and Methods* (ed. W. P. Mason), vol. 2B, pp. 265–331. Academic.

Nyborg, W. L. 1998 Acoustic streaming. In *Nonlinear Acoustics* (ed. M. F. Hamilton & D. T. Blackstock), pp. 207–231. Academic.

Otto, F., Riegler, E. K. & Voth, G. A. 2008 Measurements of the steady streaming flow around oscillating spheres using three dimensional particle tracking velocimetry. *Phys. Fluids* **20**, 093304(1–8).

Rayleigh, L. 1883 On the circulation of air observed in Kundt's tubes and some allied acoustical problems. *Philos. Trans. R. Soc. Lond.* A **175**, 1–21.

Rednikov, A. Y. & Riley, N. 2002 A simulation of streaming flows associated with acoustic levitators. *Phys. Fluids* **14**, 1502–1510.

Rednikov, A. Y., Riley, N. & Sadhal, S. S. 2003 The behaviour of a particle in orthogonal acoustic fields. *J. Fluid Mech.* **486**, 1–20.

Rednikov, A. Y. & Sadhal, S. S. 2004 Steady streaming from an oblate spheroid due to vibrations along its axis. *J. Fluid Mech.* **499**, 345–380.

Rednikov, A. Y., Zhao, H., Sadhal, S. S. & Trinh, E. H. 2006 Steady streaming around a spherical drop displaced from the velocity antinode of an acoustic levitation field. *Q. J. Mech. Appl. Math.* **59**, 377–397.

Riley, N. 1966 On a sphere oscillating in a viscous fluid. *Q. J. Mech. Appl. Math.* **19**, 461–472.

Riley, N. 1967 Oscillatory viscous flows: review and extension. *J. Inst. Math. Appl.* **3**, 419–434.

Riley, N. 1992 Acoustic streaming about a cylinder in orthogonal beams. *J. Fluid Mech.* **242**, 387–394.

Riley, N. 1997 Acoustic streaming. In *Encyclopedia of Acoustics* (ed. M. J. Crocker), pp. 321–327. Wiley.

Riley, N. 2001 Steady streaming. *Annu. Rev. Fluid Mech.* **33**, 43–65.

Rosenhead, L. (Ed.) 1963 *Laminar Boundary Layers*. Oxford Clarendon Press.

Trinh, E. H. & Robey, J. L. 1994 Experimental study of streaming flows associated with ultrasonic levitators. *Phys. Fluids* **6**, 3567–3579.

Yarin, A. L., Brenn, G., Kastner, O., Rensink, D. & Tropea, C. 1999 Evaporation of acoustically levitated droplets. *J. Fluid Mech.* **399**, 151–204.

Yarin, A. L., Pfaffenlehner, M. & Tropea, C. 1998 On the acoustic levitation of droplets. *J. Fluid Mech.* **356**, 65–91.

Zhao, H., Sadhal, S. S. & Trinh, E. H. 1999*a* Internal circulation in a drop in an acoustic field. *J. Acoust. Soc. Am.* **106**, 3289–3295.

Zhao, H., Sadhal, S. S. & Trinh, E. H. 1999*b* Singular perturbation analysis of an acoustically levitated sphere: flow about the velocity node. *J. Acoust. Soc. Am.* **106**, 589–595.